UNIVERSIDAD NACIONAL AUTÓNOMA DE MÉXICO

PROGRAMA DE MAESTRÍA Y DOCTORADO EN INGENIERÍA
INGENIERÍA CIVIL – ESTRUCTURAS

AN EXPERIMENTAL STUDY ON PRECAST REINFORCED CONCRETE BEAM-COLUMN CONNECTIONS

TESIS
QUE PARA OPTAR POR EL GRADO DE:
MAESTRO EN INGENIERÍA

PRESENTA:
VLADIMIR ENRIQUE RODRÍGUEZ MORENO

TUTOR PRINCIPAL:
DR. HÉCTOR GUERRERO BOBADILLA, INSTITUTO DE INGENIERÍA, UNAM

CIUDAD DE MÉXICO, JULIO 2019

JURADO ASIGNADO

Presidente:	DR. SERGIO MANUEL ALCOCER MARTÍNEZ DE CASTRO
Secretario:	DR. JOSÉ ALBERTO ESCOBAR SÁNCHEZ
Vocal:	DR. HÉCTOR GUERRERO BOBADILLA
1er suplente:	DR. ADRIÁN POZOS ESTRADA
2do suplente:	DR. MARCOS MAURICIO CHÁVEZ CANO

Lugar donde se realizó la tesis:

INSTITUTO DE INGENIERÍA, UNAM.

TUTOR DE TESIS:

_____

DR. HÉCTOR GUERRERO BOBADILLA

To my parents Olga Moreno and Joaquin Rodríguez

ACKNOWLEDGMENTS

Firstly, I would like to express my gratitude to Dr. Héctor Guerrero Bobadilla for his guidance and encouragement when developing this thesis; for sharing his knowledge with enthusiasm; and for giving me the opportunity to work under his supervision. Also, I want to thank the members of my thesis committee: Dr. Sergio Manuel Alcocer, Dr. José Alberto Escobar Sánchez, Dr. Adrián Pozos Estrada and Dr. Marcos Mauricio Chávez Cano, for their valuable comments that enriched this work.

My utmost gratitude to the Universidad Nacional Autónoma de México (UNAM), and its professors, for their never-ending generosity towards me since CCH-Naucalpan, through FES-Acatlán, all the way to the master's program in the CU.

I am grateful for the financial support provided by Consejo Nacional de Ciencia y Tecnología (CONACyT) through the Graduate Scholarship Program.

ABSTRACT

Precast reinforced concrete systems have many advantages over conventional cast-in-place concrete structures. Precast systems enable fast and effective construction of a wide variety of structures, making them an attractive option for building developers. However, despite their well-known benefits, these systems have been widely questioned in seismic regions, mostly attributed to lack of knowledge about said systems. As a consequence, most design codes include only general provisions for precast structures and impose heavy restrictions on their design and construction that consequently lead to discourage their use. The main focus of this work is to evaluate, based on experimental data, the seismic performance of different precast concrete beam-column connections that emulate monolithic behavior. The experimental program consisted in testing one monolithic and several precast connections subjected to simulated seismic loads. Precast connections were fabricated using different detailing, various levels of confinement, and post-tensioning. Strength and deformation capacity, energy dissipation, and stiffness degradation are assessed. Results of this study indicate that precast beam-column connections have acceptable behavior compared to conventional monolithic connections. As a secondary objective, stiffness modification factors recommended in design codes are revised and compared to results obtained experimentally. It is shown that design codes underestimate stiffness degradation in concrete members. Finally, two mathematical models were proposed to estimate the observed stiffness degradation on beam-column connections.

RESUMEN

Los sistemas de concreto prefabricado tienen algunas ventajas interesantes sobre estructuras convencionales coladas en sitio. Los sistemas prefabricados permiten la rápida y eficiente construcción de una variedad de estructuras, haciéndolos atractivos para desarrolladores de edificios. Sin embargo, a pesar de estas muy conocidas ventajas, el uso de estos sistemas ha sido cuestionado en zonas sísmicas, principalmente por la falta de conocimiento sobre éstos. Como consecuencia, los códigos de diseño generalmente sólo incluyen especificaciones generales para estructuras prefabricadas e imponen restricciones severas para su diseño y construcción que finalmente desmotivan su uso. El objetivo principal de este trabajo es evaluar, basado en datos experimentales, el desempeño sísmico de distintas conexiones viga-columna de concreto prefabricado. El programa experimental consistió en someter una conexión monolítica y varias conexiones prefabricadas, que emulan comportamiento monolítico, a cargas cíclicas reversibles. Los resultados se presentan en términos de resistencia y capacidad de deformación, disipación de energía, y degradación de rigidez. Las conexiones fueron fabricadas con distintos detallados, varios niveles de confinamiento, y postensado. Los resultados de este estudio indican que las conexiones viga-columna de concreto prefabricado tienen comportamiento aceptable comparadas con conexiones monolíticas convencionales. Como segundo objetivo, los factores de modificación de rigidez de algunos códigos son revisados y comparados con los resultados obtenidos experimentalmente. Se demuestra que los códigos de diseño subestiman la degradación de rigidez de elementos de concreto. Finalmente, se propuso un modelo matemático que permite evaluar la degradación de rigidez observada en conexiones trabe-columna.

LIST OF CONTENTS

LIST OF FIGURES

LIST OF TABLES

CHAPTER 1

INTRODUCTION

1.1 BACKGROUND

Precast concrete systems have numerous advantages over conventional cast-in-place concrete structures, to name a few: higher quality control obtained in precast plants, faster erection, and aesthetic architectural shape of the members [1, 2]. They also offer a wide variety of fabrication and assembly options that are solely limited by fabricator capabilities and the designer´s or contractor´s comfort in using these systems [3]. Given these advantages, reinforced concrete precast systems (RCPS) are an attractive alternative to building developers. However, despite these well-known benefits, these systems have been widely questioned in seismic regions [3]. Although some criticism may be based on negative past experiences, such as the 1995 Kobe and 1988 Armenia earthquakes where many precast buildings structures failed [35], it seems that most questions are attributed to lack of knowledge of these systems. More often than not, poorly designed and constructed precast structures have performed inadequately due to brittle (non-ductile) behavior of poor connection details between precast members, poor detailing, and poor design concepts [36]. As a consequence, most design codes (e.g. [4, 5]) include only general provisions for precast structural systems and impose heavy load factors and restrictions on precast construction that subsequently lead to discourage their use. However, based on this study and others, these restrictions appear to be excessive when it has been seen that strength and deformation capacity of precast connections are equivalent to those of cast-in-place connections.

Precast concrete frames are constructed assembling the precast beams and columns on site, and are connected by means of emulated monolithic connections and non-emulated ones. As a result, beam-column connections of moment resisting frames may be vulnerable to severe lateral loading such as earthquakes [6]. The challenge, hence, in precast

construction lies in finding economical and practical methods of connecting precast elements together that guarantee acceptable stiffness, strength, ductility and stability [2]. Detailing and structural behavior of the connection affect these aspects as well as the constructability and load distribution [7]. Moreover, effective design and construction is attained through the use of suitable connections that cater for all service, environmental and ultimate load conditions [8].

Given modern day requirements for building design and construction, the performance-based seismic design philosophy is being adopted worldwide [9]. Such philosophy consists in producing buildings capable of achieving predefined performance objectives considering a potential range of future ground motions. Performance objectives are thresholds associated to different states of damage, which can be expressed in terms of inter-story drifts for each seismic intensity. Generally, in order to achieve certain performance levels, non-linear analysis is conducted for the seismic-force-resisting system [9]. However, reinforced concrete structures behave unpredictably under seismic movements, demanding post-cracking and post-yielding stresses, making it difficult to analytically represent these conditions. Therefore, experimental tests on seismic-force-resisting systems are essential in order to understand inelastic behavior of concrete structures. This thesis aims to assess experimental results obtained from tests applied to precast reinforced concrete (RC) beam-column connections under simulated seismic loads.

Results of an experimental project carried out at the National Autonomous University of Mexico (UNAM) in conjunction with the Large Structures Laboratory of the National Disaster Prevention Center (CENAPRED) are presented and discussed in this thesis. The primary objective of this investigation is to evaluate, based on experimental data, the seismic performance of different connection types of precast reinforced concrete members. Comparisons among a benchmark monolithic connection and several precast beam-column joints are presented in terms of strength and deformation capacity, energy dissipation, and stiffness degradation. After testing, the monolithic connection was repaired using carbon fiber reinforced polymer and re-tested.

Precast specimens were designed to emulate monolithic construction and to develop a strong column-weak beam mechanism. Beam-column connections (similar to those in [6,

10]) were fabricated using different detailing, various levels of confinement, and post-tensioning. It is significant to mention that specimens were tested at full-scale. Columns had cross-sectional dimensions of 600x600 mm, while beams were 450x810 mm. A total of seven beam-column connections were tested, six of them being precast specimens.

A relation between effective stiffness and inter-story drift, as well as visible damage on elements, is reported. With this data, an effective stiffness model for reinforced concrete beams is proposed. Such model can be refined and used to consider specific connection or section types if needed. It was found that stiffness modification factors for cracked beam sections recommended in design codes (e.g. [4, 5, 11]), underestimate the level of degradation that concrete elements undergo after reaching certain drift demand.

In recent times, it has been more obvious that man-made structures located in seismic regions can be exposed to foreshocks, the mainshock (i.e. the seismic event with the largest earthquake magnitude), and aftershocks [12, 13]. In some cases, aftershocks can reach higher peak-ground accelerations than those of the mainshock [14], worsening structural damage. If stiffness modification factors are recommended for linear analysis, those should be related to the maximum permitted design drift ratios. In this way structures are not left vulnerable to aftershocks. A clear example is the February 2011 M_w 6.2 Christchurch earthquake, which was an aftershock of a sequence of earthquakes, triggered by the Darfield earthquake of September 2010, which reached higher seismic intensity levels in the city and affected many RC buildings [15].

As a matter of interest, a physical comparison of damage presented in each specimen at different drift demands is reported. This will serve as an aid for engineers on the types of damages expected when buildings reach design drifts recommended by codes. Also, the effective stiffness model, proposed in this thesis, will help designers predict the expected structural damage on members beyond the design drift limit.

Based on the experimental results we cannot conclude that the response of the precast specimens was superior compared to the monolithic specimen. However, consistent with the literature review findings, the beam-column connections showed acceptable performance when compared to the monolithic counterpart.

1.2 OBJECTIVES AND SCOPE

The main objective of this thesis is to evaluate the performance of precast reinforced concrete beam-column connections under slowly applied (quasi-static) loading and compare the results with the behavior of a conventional monolithic connection.

Specific objectives of this study are: 1) understand the advantages and disadvantages of precast connections in seismic regions and promote their use once their capacities are known; 2) revise stiffness modification factors recommended in design codes and compare them with the experimental results; and 3) propose an effective stiffness model that correlates stiffness degradation with inter-story drift demands.

The research was developed with the following scope:

1. One benchmark monolithic connection and six precast connections were tested under simulated seismic loading.
2. Test setup and loading protocols were based on the specifications in [9], limited to quasi-static loading.
3. The effective stiffness model proposed is empirical, based solely on experimental results and is limited to concrete connections with rectangular cross-sections.

1.3 OUTLINE OF THE THESIS

This thesis contains six chapters where this introduction serves as the first one. The following paragraphs present a general description of the content of each following chapter.

Chapter 2 is a literature review of related topics concerning precast RC beam-column connections such as studies from various researchers and basic provisions in design codes.

Chapter 3 describes the experimental program including a detailed specimen description (geometry and materials), fabrication specifics, test setup, instrumentation and loading protocol.

In Chapter 4, experimental results are presented, namely: load-deformation and energy dissipation curves, and an extensive comparison of cracking presented on each specimen.

Chapter 5 proposes two effective stiffness models based on the experimental data obtained: a general model and a simplified bilinear model. Also, results are compared to the stiffness modification factors presented in Chapter 2.

Finally, Chapter 6 presents conclusions and recommendations for future work to be developed after this thesis.

CHAPTER 2

LITERATURE REVIEW

2.1 PRECAST CONCRETE CONNECTIONS

From a design perspective, as mentioned in [3], precast concrete frames can be divided into two categories: those that emulate cast-in-place concrete construction (emulative) and those that provide connections that are able of sustaining post-yield deformations (non-emulative or yielding). For the emulative approach, post-yield rotations are expected to occur on the concrete beam away from the region where precast members are connected. This is achieved by using systems similar to the one presented in Fig. 2-1, were post-tensioning is combined with conventional reinforcement in order to force the plastic hinge away from the connection; and Fig. 2-2, where the beam is spliced at a practical length with a mechanical or wet connection away from the plastic hinge region. However emulative systems seldom progress beyond the prototype due to their excessive cost of development [3].

Many strong nonyielding connections have been proposed for use in seismic regions. French et al. in 1989 [16] developed connectors using post-tensioned bars, designed to force yielding away from de beam-column interface. Ochs and Ehsani [17] proposed beam-column connections using two welded connections that relocate the plastic hinge away from the column face and caused cracking in the beam region, which is a desirable characteristic for seismic design.

Yielding connectors on the other hand allow the joining of precast elements at the beam-column interface. They are likely able to allow larger deformation limit states and produce less earthquake damage as they tend to yield at loads that are below the yield strength of reinforcing bars, thus absorbing more energy [3].

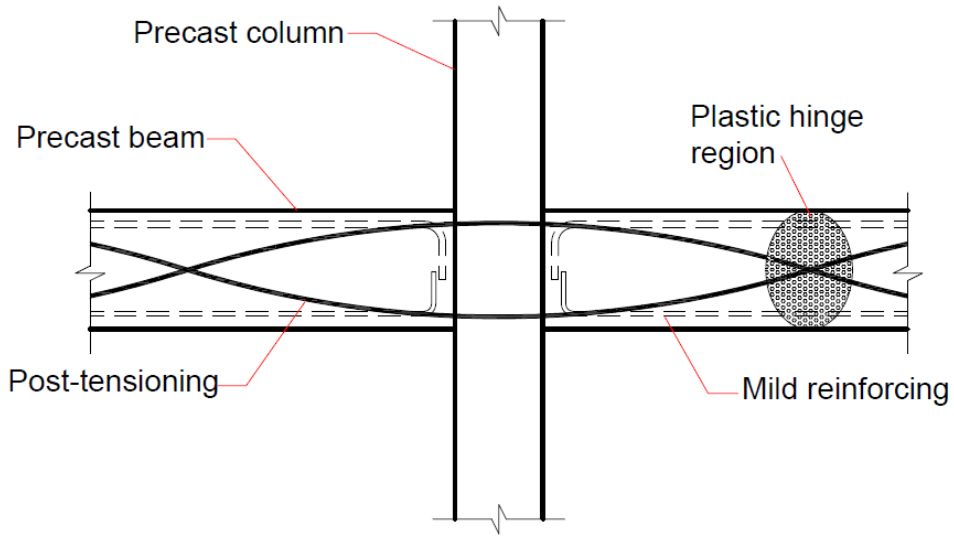

Figure 2-1. Strong nonyielding beam-column connection.

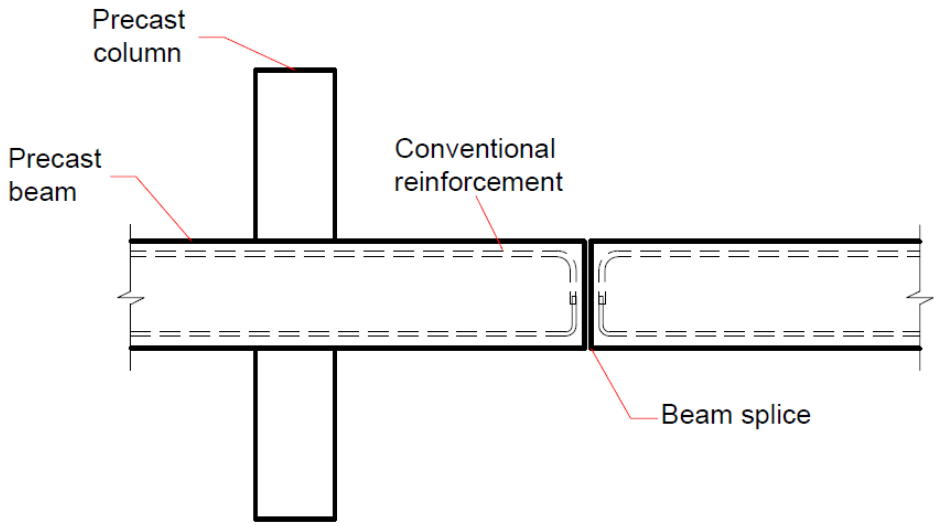

Figure 2-2. Continuous beam system.

In cast-in-place concrete, the postyield rotation occurs over a plastic hinge region, as shown in Fig. 2-3, and the strain in concrete and reinforcing steel is considered constant and extends some distance past the plastic hinge region [3]. The difference with precast systems is that when members are joined at the face of the column, a weakened plane or discontinuity is created, where a significant portion of the rotation occurs. Inelastic deformations are

concentrated in the region where a “crack” already exist between the precast members [18]. Moreover, emulative connections develop the strength of the reinforcing bars at the beam-column interface.

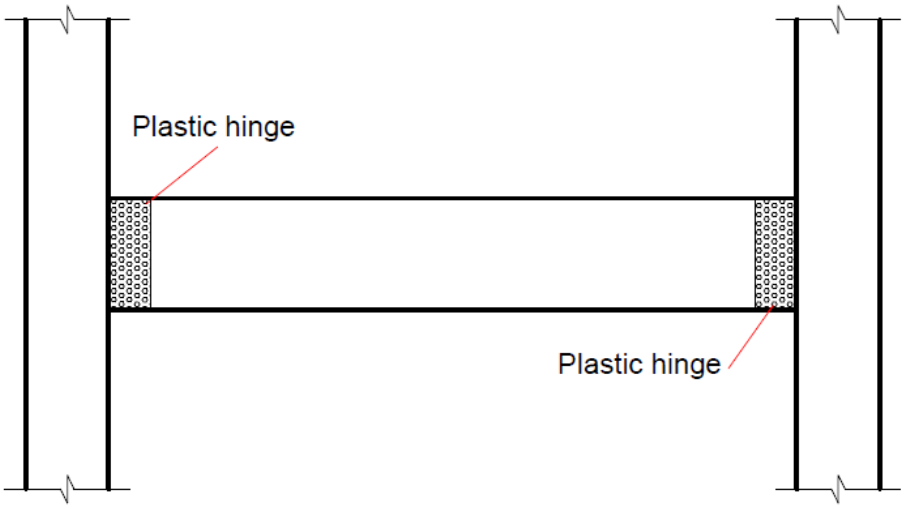

Figure 2-3. Cast-in-place frame system.

2.2 EXPERIMENTAL STUDIES ON PRECAST CONCRETE SYSTEMS

A number of important studies have been conducted to evaluate the seismic response of precast concrete beam-column connections. Palmieri et al. [1] devoted important research and development to provide precast systems with stable plastic behavior, finding that beam-column connections can be detailed to exhibit suitable behavior when used in lateral force resisting systems designed for seismic regions. Park et al. [6] investigated the earthquake resistance of precast U-shaped beam-column connections. Test results showed that the beam-column connections had acceptable strength and deformation capacity, however, energy dissipation was decreased due to bond-slip of the reinforcing bars inside the U shell. Also, shear crack and shear deformation of the beam-column connection were increased.

In 1995, Loo and Yao [7] evaluated the behavior of two types of precast beam-column connections. A total of 18 half-scale specimens (including six monolithic connections) were tested under static and cyclic loading. All models had the same dimensions but different groups had different concrete strengths and/or steel ratios. Axial loading was applied at the

top of the column. Vertical loading was applied at the beams end sequentially until failure. Under both static and cyclic loading, crack propagation and failure crack patterns were mainly similar in all specimens. Also precast connections attained higher flexural strength than the monolithic connections. Precast connections, under cyclic loading, had adequate ductility characteristics and possessed larger energy-absorbing capacities when compared to their monolithic counterparts.

El-Sheikh et al. [18] discussed the behavior and design of unbonded post-tensioned precast concrete frames developing ductile frames in which the nonlinear/inelastic deformations occured only in the connections. Hence, behavior of the precast frame was controlled by the beam-column connection behavior.

As an alternative to monolithic emulation, Nakaki et al. [19] developed ductile connectors that exploit the inherent attributes of precast concrete systems. These connectors contain rods that yield at well-defined strengths that limit the loads that can be transferred to less ductile components of the frame. In 2006, Ertas et al. [20] tested one monolithic specimen and four types of ductile connections, three of which presented strength properties and energy dissipation capacity suitable for seismic zones and had hysteresis behavior similar to that of the monolithic connection. This study showed that the bolted connection had superior performance combined with fabrication ease and assembly.

In more recent years, Parastesh et al. [21] also devoted research in developing a new ductile moment resisting connection suitable for seismic zones. Their proposed system enables fast construction and eliminates the need for formworks, bolting, welding and prestressing. The precast columns of the system were cast continuously with a free space in the connection zone where four diagonal bars were placed to provide adequate strength and stability. The precast beams, in the connection zone (i.e. the plastic hinge zone, calculated to be 600 mm), had a hollow U-shaped cross section. A longitudinal bar was used in the precast U section to support diagonal stirrup bars. Bottom longitudinal reinforcement was spliced in the cast-in-place area of the beam and top reinforcement bars were continuous through the beam-column joint and are fixed to the precast beams outside the connection with a layer of grout. Experimental results of this study showed that the proposed connections had: higher flexural strength and initial stiffness compared to similar monolithic specimens, acceptable

stiffness degradation up to 4% drift, flexural cracks were mainly concentrated in the plastic hinge zone of the beams, diagonal reinforcement in the joint core of the connections delayed development of diagonal cracks, the precast connections exhibited higher ductility ratios and, for similar drifts, dissipated up to 30% more hysteretic energy compared to monolithic specimens.

As for experimental studies on large scale precast concrete buildings, in 1999, Priestley et al. [22], as the culmination of the 10-year Precast Seismic Structural Systems (PRESSS) research program, tested a 0.60-scale five-storey precast building under simulated seismic loading. Seismic input was at least 50% higher than those required for Uniform Building Code (UBC) Seismic Zone 4. The design of the building was conducted with concepts developed during the PRESSS research program which can be consulted in [23]. Also, an in depth description of the building design is described in [24]. The building comprised four different ductile structural frame systems (prestressed and non-prestressed) in one direction, and a jointed wall system in the orthogonal direction. The main method of testing the building was pseudodynamic testing using spectrum-compatible earthquake segments. Lateral forces and displacements were applied by two actuators at each floor level. Results of this study were more than satisfactory. Damage in the wall direction was minimal with minor spalling at the wall base and flexural cracking. In the frame direction, damage was significantly less than could be expected for similar RC structures at similar drift levels. Drift demand reached 4.5%. Both prestressed and non-prestressed frames performed well, however, the latter had slightly more damage than the former. Overall crack levels due to shear in beam-column joints were extremely small despite being subjected to high seismic intensities.

In an effort to combine the benefits of precast construction with seismic protection systems, Guerrero et al. [25] evaluated the effects of Buckling-Restrained-Braces (BRBs) on precast models subjected to earthquake ground movements. Two four-story reinforced concrete models were studied under shaking table excitation. One model was a conventional precast frame system designed according to common practice in Mexico, while the other was equipped with BRBs and designed using a performance-based methodology proposed in [26]. Results of this investigation showed that BRBs can effectively improve the behavior of

precast structures maintaining them elastic, and therefore presenting minimal damage in the beam-column connections even when exposed to major earthquakes. Inter-story drifts and lateral displacements in the model equipped with BRBs where approximately half of those in the unequipped model. Also, the use of BRBs delayed and reduced stiffness degradation of the structural members. BRBs were found to be an excellent option to provide earthquake-resistance to precast buildings maintaining all their advantages while using standard detailing. The beam-column connections presented in this study are sub-assemblages of the models discussed in [25], as it is described later in Chapter 2.

2.3 MEXICO CITY BUILDING CODE AND ACI-318-14

2.3.1 Precast structures

As mentioned above, there are two alternatives for the design of precast lateral force resisting systems. One approach is the use of the unique properties of the precast concrete elements interconnected by dry or wet connections [27]. The other alternative is by emulation of monolithic RC construction. The latter is more commonly used in codes [2]. The objective of emulated monolithic connections is to make the connection as strong as the cast-in-place connection [6].

The México City Building Code (MCBC) and its complementary specifications [4, 5] bases its regulations of precast concrete systems on emulation of monolithic cast-in-place structural systems. Hence, all precast systems are designed with the same criteria as specified for cast-in-place structures.

The 2004 version of the MCBC [4] requires that connections of the structural system have to be designed to resist 1.3 times the design forces and moments obtained in analysis, this in addition to the usual load factors. The more recent 2017 version of the MCBC [5] adds a factor of 1.4 for column-to-column connections. Yielding stress of the steel reinforcement in connections is limited to 412 MPa. The specified concrete compressive strength f_c', used in connections that join precast elements, must be no less than that of the adjoining elements.

All precast structures have to be designed under earthquake induced forces. The MCBC seismic design criteria is mainly force-based, hence earthquake induced forces are

related to the structural ductility achieved through seismic response modification factors, Q. For precast concrete moment resisting frames, a Q of 2 or 3 is used. Forces calculated with this method are considerably less compared to those expected if the structure were to perform in the elastic range.

2.3.2 Cracked stiffness of concrete elements

Under service conditions, concrete structures will suffer stiffness degradation because of cracking, which can lead to amplified lateral displacements when subjected to ground motion. In a modal analysis, the fundamental period of vibration would be determined as if all structural elements (beams, columns, walls) present no cracking whatsoever, and consequently lead to incorrect seismic forces. As a result, it is important to consider the cracked stiffness of the structural elements. A simplified method, adopted by most design codes [4, 5, 11], consist in using reduction factors on the moments of inertia of the gross cross-sections.

When linear analysis methods are used to determine stiffness of structural elements, the effects of cracking will be taken into account. The cracked stiffness of a structural element will be calculated using the modulus of elasticity of concrete, E_c, and the moments of inertia presented in Table 2-1. A comparison of the modification factors used in ACI-318-14 Building Code Requirements for Reinforced Concrete [11] is also shown in Table 2-1.

Table 2-1. Modifications factors for cracked stiffness.

Structural element	MCBC	ACI
Beams	*0.5Ig*	*0.35Ig*
Walls	*0.5Ig*	*0.35Ig*
Walls (uncracked)	*Ig*	*0.7Ig*
Columns	*0.7Ig*	*0.7Ig*

Factors used from the MCBC do not take into account the shape of the section, steel reinforcement or axial loads on columns [28]. That said, neither do those shown in ACI, however, this code does offer the option of using alternative equations for calculating the cracked stiffness (see Table 2-2) in order to consider the aforementioned issues. Also, both

design codes recommend these factors regardless of the structural system, whether it be precast o cast-in-place concrete.

Note that ACI specifies a smaller factor of $0.35I_g$ for beams, while the MCBC has a factor of $0.5I_g$. Additionally, the ACI code specifies minimum and maximum values for *I* when using equations from Table 2-2.

Table 2-2. Alternative values for cracked stiffness.

Element	Minimum	*I*	Maximum
Columns and walls	*0.35Ig*	$\left(0.8+25\frac{A_{st}}{A_g}\right)\left(1-\frac{M_u}{P_u h}0.5\frac{P_u}{P_0}\right)I_g$	*0.875Ig*
Beams	*0.25Ig*	$(0.1+25\rho)\left(1.2-0.2\frac{b_w}{d}\right)I_g$	*0.5Ig*

2.3.3 Maximum drift ratios for concrete structures

Table 2-3 shows the MCBC's [5] maximum inter-story drifts (γ_{max}) permitted for conventional and precast frame buildings in function of the expected ductility. It should be noticed that this code does not include a high ductility value for precast frame buildings (i.e. Q=4), however the two maximum drifts allowed for these systems are the same for conventional cast-in-place concrete structures for medium and low ductile buildings.

Table 2-3. Seismic response factors and maximum drifts for concrete structures.

Structural System	Ductility	*Q*	γ_{max}
Frame building	High	4	0.030
	Medium	3	0.020
	Low	2	0.015
Precast frame building	Medium	3	0.020
	Low	2	0.015

ASCE/SEI 7-16 [29] specifies maximum drift ratios depending on the risk category of the structure (see Table 2.4), having I and II a low risk to human life in the event of failure, III having a substantial risk to human life, and IV being all buildings and other structures

considered essential facilities. Table 2.4, however, does not make a distinction with precast and cast-in-place concrete structures.

Table 2-4. Maximum drift ratios for ASCE/SEI 7-16 [29].

Risk Category	Drift
I or II	0.020
III	0.015
IV	0.010

While the MCBC does make a distinction between precast and cast-in-place concrete buildings, neither of these codes make a direct relation between the maximum inter-story drifts permitted and the modification factors presented in section 2.3.2. If, in a seismic event a structure reaches certain drift, it will lose significant stiffness, leaving it vulnerable to aftershocks that in some cases can have a higher peak-ground acceleration than the main shock. Despite this problem, modification factors are the same regardless of the design drift limit. In this study, a relation between inter-story drift and stiffness degradation was found experimentally; which contradicts code recommendations.

CHAPTER 3

EXPERIMENT SETUP

3.1 SPECIMEN DESCRIPTION

Seven full-scale bean-column connections with different detailing, levels of confinement and post-tensioning were tested under cyclic loading. As mentioned above, tested specimens were sub-assemblages from a prototype four-story precast reinforced concrete buildings (Fig. 3-1a) studied by Guerrero et al. [25]. These models were designed using the MCBC-2004 [4] and were assumed to be located in the lakebed zone of Mexico City. Connections were not designed to resist 1.3 times the design forces. However, in a real design case this should be taken into account as stated in section 2.3.1.

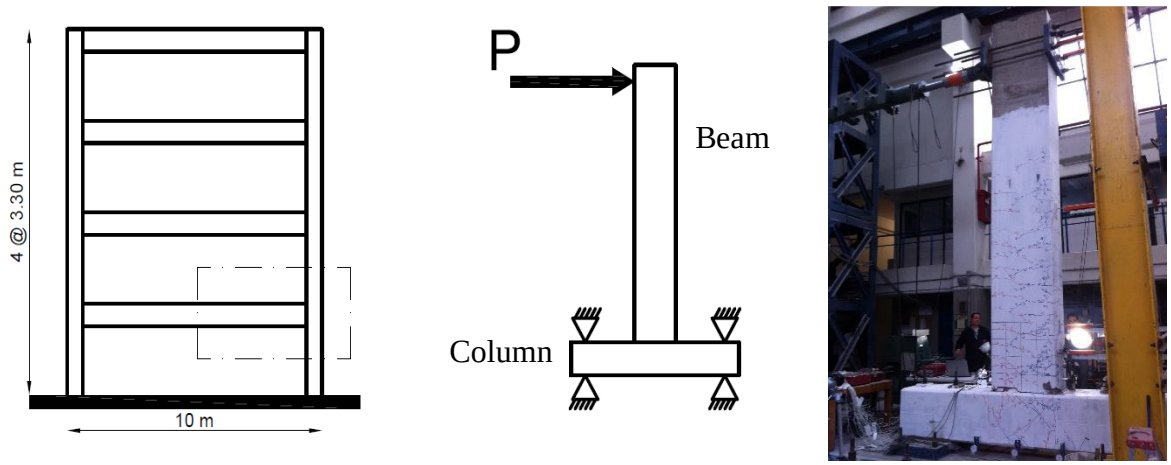

a) Prototype structure b) Specimen scheme and setup

Figure 3-1. Prototype structure and specimen scheme.

Test specimens were an exterior connection that represented the region from mid-column height below and above the connection, and to mid-span of the beam. The column had a length of 3.3 m and the beam a length of 5.0 m. Beams were oriented vertically while

columns laid horizontally (Fig. 3-1b). Cyclic lateral loads were applied at the extreme end of the beam. No axial load was applied to columns since the analysis of the prototype structure studied by Guerrero et al. [25] showed that the axial load was less than 10% of the columns' compressive strength. Also, experimental evidence suggests that axial load has no effect on joint shear strength [31]. All specimens were connected to the reaction slab at both column ends, providing limited rotational restraint simulating a hinged support. A similar test setup can be found in [32]. Results presented herein should be interpreted taking into account these limitations.

For comparison reasons, a total of seven specimens were fabricated. The test subjects consisted of one monolithic connection (Fig. 3-2b); three conventional precast connections (Fig. 3-2c, d and e); two post-tensioned precast hybrid connections (Figs. 3-2f and g); and one precast connection where the beam was supported on a column bracket (Figs. 3-2h). All precast specimens are U-shaped with a cast-in-place core. Precast beams had the same cross-section dimensions. However longitudinal and transverse reinforcement varied in order to analyze the effects on connection performance. For beams, longitudinal reinforcement consisted of 4#8 bars at the beam's bottom and 2#12 bars at the top (except Specimens 5 and 6, which consisted of 3#8 bars at the beam's bottom and 2#10 bars at the top), while transverse reinforcement consisted of #3 stirrups with varied spacing. Columns, on the other hand, were the same for all specimens (see Fig. 3-2a). All test specimens are described in Table 3-1.

Table 3-1. Description of test specimens.

Specimen	Description	Stirrups spacing, mm
1	Monolithic	300
1-R	Monolithic repaired	300
2	Precast 1	300
3	Precast 2	150
4	Precast 3	75
5	Precast post-tensioned 1	150
6	Precast post-tensioned 2	75
7	Precast with bracket	150

Specimen 1, i.e. the monolithic specimen, was retested after rehabilitation using carbon fiber reinforced polymer (CFRP). To cover the plastic hinge cracks formed during the first test, one layer of fiber in the longitudinal direction and one in the transverse direction were located. While the former had a length of two effective depths (d_e), the latter had a length of 1.5 effective depths. These lengths were considered in order to cover most of the plastic hinge cracks (which appeared during the first test and within one effective depth).

Precast connections were fabricated using a precast U-shaped beam with bottom longitudinal reinforcement placed on top of the precast flange, which led to a smaller effective depth compared to the monolithic connection. Spacing of stirrups for precast connections were 300, 150 and 75 mm for Specimens 2, 3 and 4, respectively.

Specimens 5 and 6 consisted of a precast post-tensioned hybrid connection. Post-tensioning was applied using 6-13 mm strands, and a 25 mm thick steel plate as shown in Figs. 3.2f and 3.2g. A total force of 440 kN was applied on the strands, which represented a stress of 1.2 MPa or 2.2% of the concrete's compressive strength. Spacing for stirrups were 150 and 75 mm for Specimens 5 and 6, respectively.

Specimen 7 was a proposed alternative beam-column connection, which was supported on a concrete bracket. Support consisted of a steel plate (PL1) welded to three #10 L-shaped rebars that extend into the column joint (see Fig. 3-3). The beam soffit also had a steel plate (PL2) that was welded to PL1 in order to transfer moment forces. The beam's top reinforcement extended inside a column gap by means of 90-deg hooks and was placed once the beam was supported by the column's bracket.

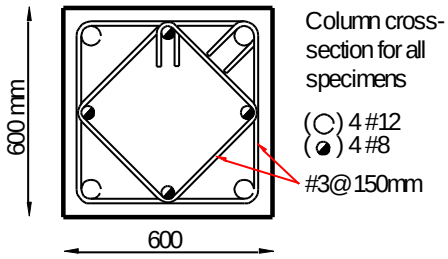

a) Column

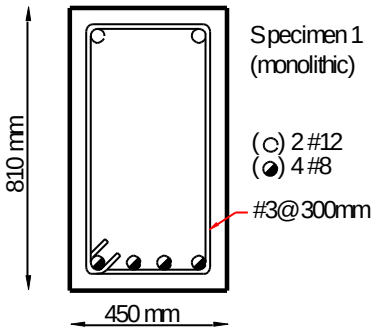

b) Beam 1

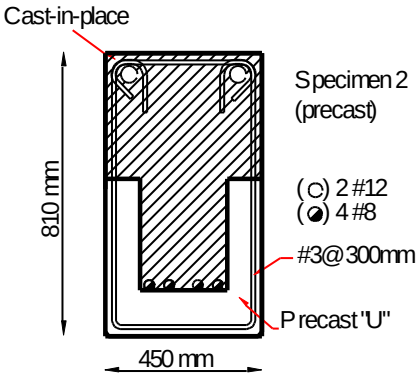

c) Beam 2

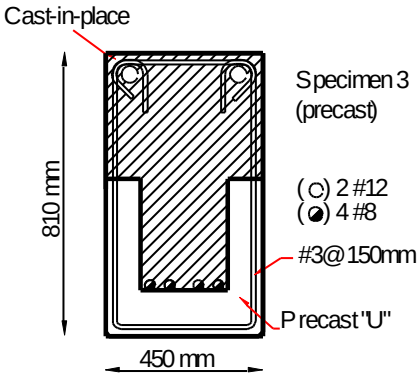

d) Beam 3

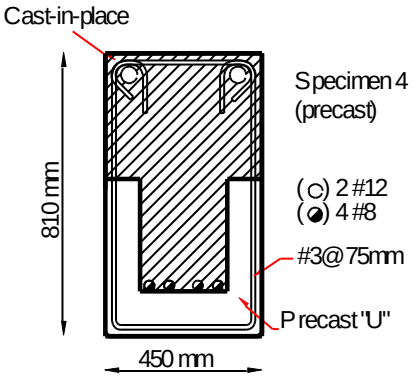

e) Beam 4

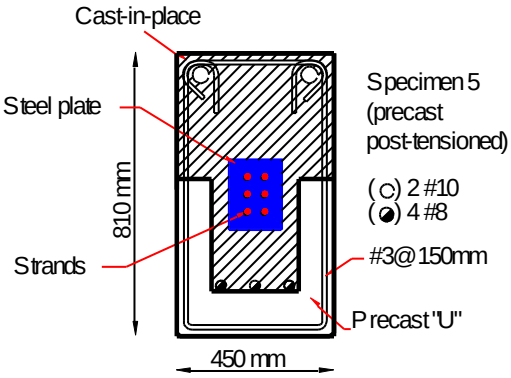

f) Beam 5

Figure 3-2. Specimen characteristics (continues).

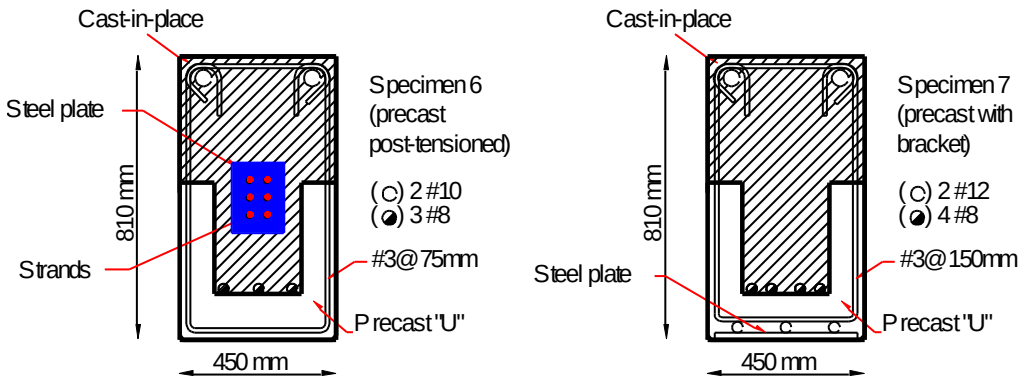

g) Beam 6 h) Beam 7

Figure 3-2. Specimen characteristics.

Specimens were made of concrete (with an average compressive strength of 55.2 MPa obtained from cylinder test sampled during concrete casting) and reinforced with low-carbon bars with a specified yield stress of 420 MPa. Fabrication process was as follows: the precast parts of the specimens, i.e. the columns and U-shaped beams, were made and arranged, as shown in Fig. 3-4, in order to place the longitudinal reinforcement and finally locate the cast-in-place concrete. Columns had open gaps to allow placement of the precast beams during assemblage. It is worth mentioning that this precast procedure improves construction speed mainly for two reasons: 1) U-shell precast beams are provided with pre-stressed strands (which make them auto-supportable and help to avoid intermediate supports); and 2) rapid cure concrete is used in the wet connections (which reaches a resistance around 25 MPa within 12 hours and allows a smooth working process, i.e. if a concrete pour is carried out in an afternoon, works can continue the next morning).

Specimens were designed using equations from the MCBC [4]. For the beams, the resistance factor F_r was considered as 1 and the expected yield stress of steel reinforcement as $1.1f_y$, due to this being an experimental study. It should be noted that the precast beams have smaller effective depths due to the U-shaped section, and therefore lower strengths compared to the monolithic beam.

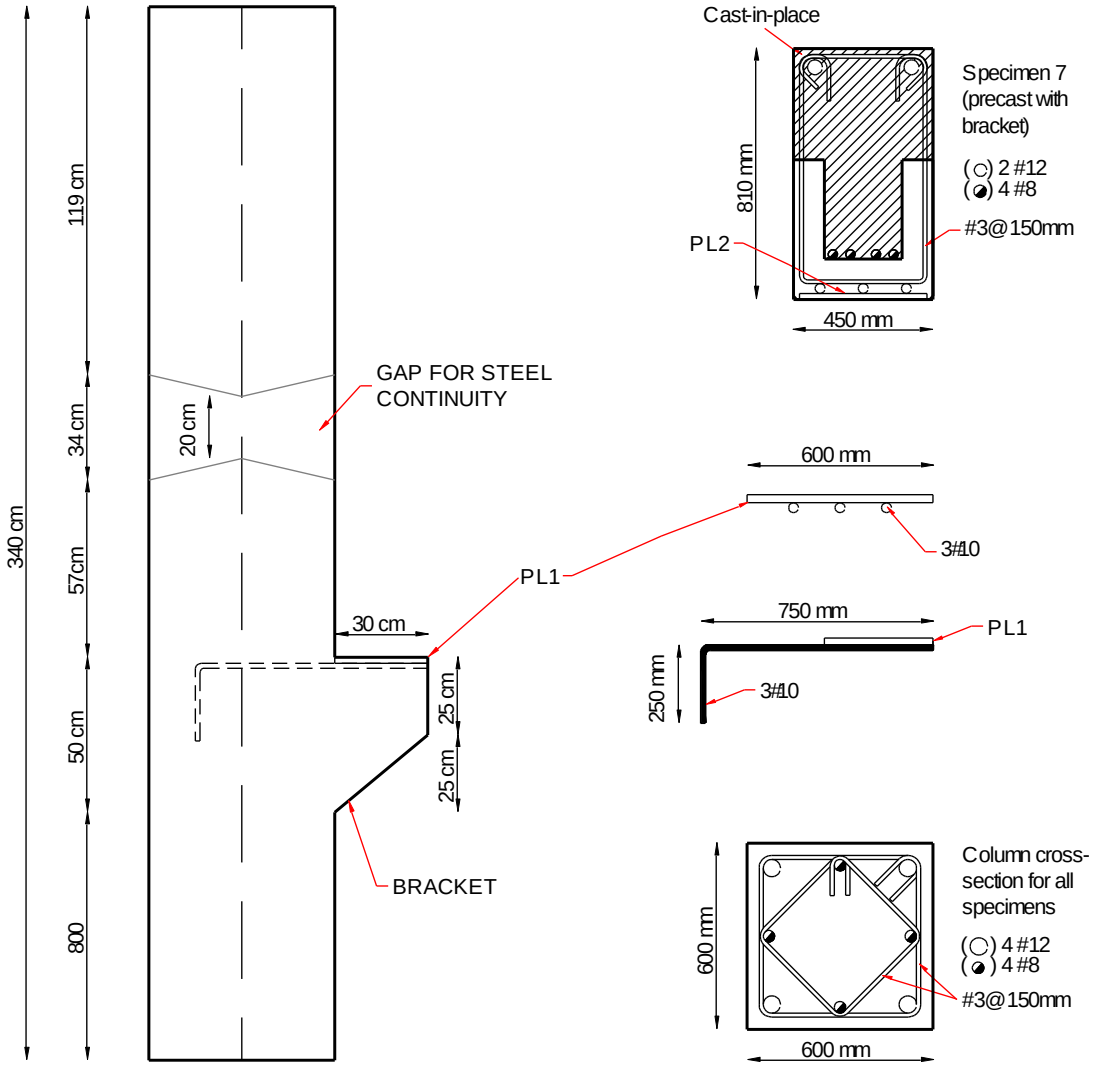

Figure 3-3. Characteristics of specimen 7.

A nonlinear analysis determined that yielding takes place at an approximate displacement of 3.5 cm. The expected yielding load is 157 kN, which is slightly higher than the results obtained in the linear analysis using equations from [4] described above.

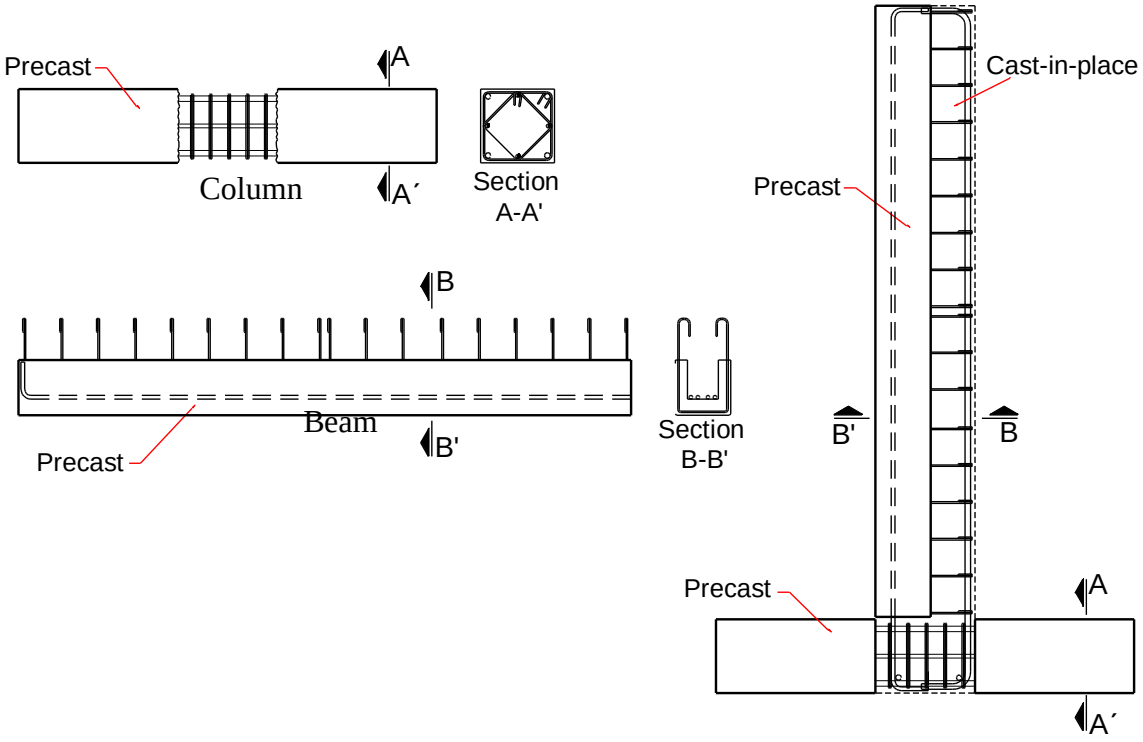

Figure 3-4. Beam-column connection.

3.2 INSTRUMENTATION

In order to measure deformations, displacements and reinforcement strains, all specimens were instrumented. Linear variable differential transformers (LVDTs) were installed to assess local deformations and displacements as follows: a) horizontal LVDTs were placed along the beam to measure displacements; b) vertical LVDTs were placed on the beam and column to measure rotations; and c) diagonal LVDTs to measure shear deformations (see Fig. 3-5).

Electric foil strain gauges were placed on the concrete surface and bar reinforcement to assess strain distributions. A total of 28 strain gauges were used (see Table 3-2). Due to the symmetric nature of the specimens, only one of the lateral surfaces was instrumented. Also, a load cell was located in the actuator to register the applied loads.

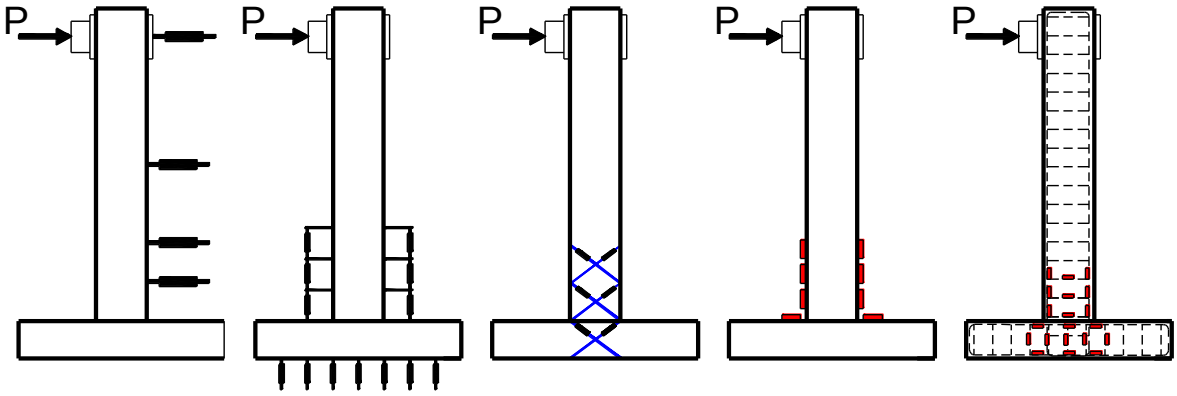

a) Horizontal LVDTs | b) Vertical LVDTs | c) Diagonal LVDTs | d) Strain gauges on concrete | e) Strain gauges on steel bars

Figure 3-5. Instrumentation of specimens**.**

Table 3-2. Location of strain gauges.

Gauges	Location
8	Beam longitudinal reinforcement.
3	Beam transverse reinforcement.
6	Column longitudinal reinforcement.
3	Column transverse reinforcement.
6	Beam concrete.
2	Column concrete.

3.3 LOADING PROTOCOL

ACI 374.2R-13 testing protocol was followed [9]. Said protocol consisted of slowly applied (quasi-static) loading. First, small load controlled cycles were applied to the specimens in order to measure initial stiffness. Cycles to 42, 63, 83 and 108 kN were applied whilst the expected yielding load was previously calculated at 157 kN. Two cycles were applied at each load level. After that, a displacement controlled history was applied. Displacement controlled cycles applied to each specimen is shown in Fig. 3-6. Inter-story drifts, calculated as the ratio between beam tip displacement and beam length, are also shown. Note that one smaller deformation reversal was applied between each pair of cycles, at 50% the displacement reached in the previous pair, in order to re-center the specimens before applying larger deformations, and measure stiffness degradation after each significant deformation demand level. In between load applications, visual inspection, photographing, and manual marking

of cracks and their propagation were carried out. A photographic record is presented in the next chapter.

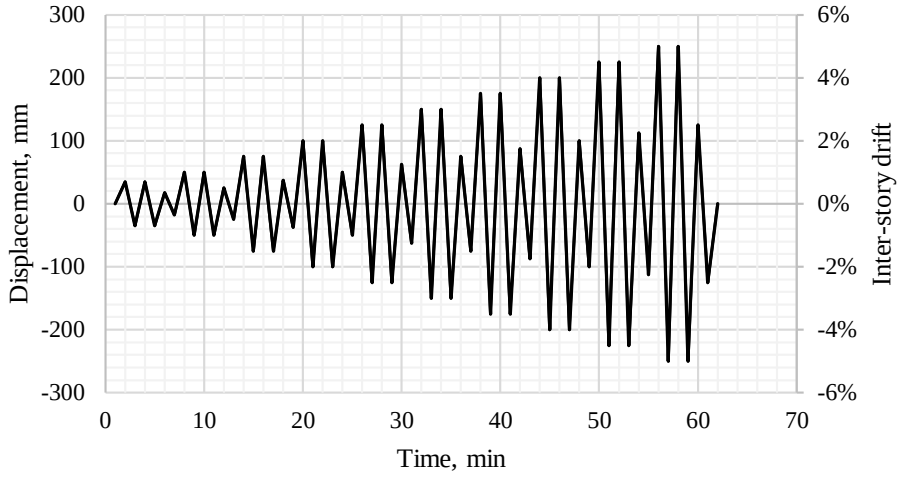

Figure 3-6. Typical displacement/drift history applied.

As it is seen in the next chapter, Specimen 1 presented significant damage at an inter-storey drift to 3%, therefore the test was terminated in order to repair the connection for re-testing. Precast specimens were taken to inter-storey drifts to 5%, and above, in order to observe their full capacity. Specimen 7, however, failed approximately at an inter-storey drift to 2.5%.

CHAPTER 4

EXPERIMENTAL RESULTS

4.1. CRACKING AND VISIBLE DAMAGE

Cracking patterns of specimens at displacements of 50, 100 and 150 mm (equivalent to inter-storey drifts to 1, 2 and 3%) are shown in Figures 4-1, 4-2 and 4-3, respectively. Specimen 7, as mentioned, failed at 2.5% drift, thus maximum crack width (w_c) shown in Fig. 4-3 was registered at said deformation demand. This physical comparison is particularly important to predict the level of damage expected at different deformation demands depending on the type of beam-column connection. Based on visual evidence, the following observations were made:

1. Specimen 1 exhibited the largest damage with severe flexural cracking, concrete crushing and even spalling. Buckling of beam longitudinal bars was observed at inter-storey drift demands to 3%
2. Precast specimens showed smaller levels of damage and this is limited to flexural and diagonal cracking. The reduced level of damage is explained by the concentration of the plastic deformation of the beam longitudinal reinforcement at the beam-column interface, where cast-in-place and precast concrete formed a cold joint.
3. Specimens 5 and 6 (post-tensioned specimens) had significantly less damage compared to the monolithic and the conventional precast connections at same drift demands. This reduction of damages can be attributed to two aspects: 1) post-tensioning of the beams; and 2) level of confinement, i.e. the stirrups smaller separation.
4. Although precast specimens presented less damage than the monolithic specimen, spalling also took place for Specimens 2, 3 and 7 as observed in Fig. 8.

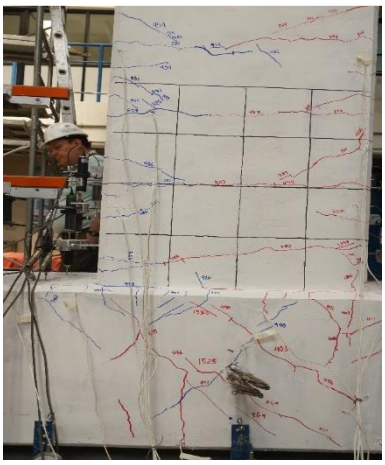

a) Specimen 1 (w_c=1.1 mm)

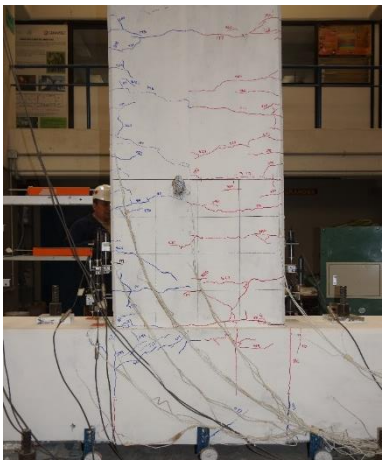

b) Specimen 2 (w_c=1.8 mm)

c) Specimen 3 (w_c=1.8 mm)

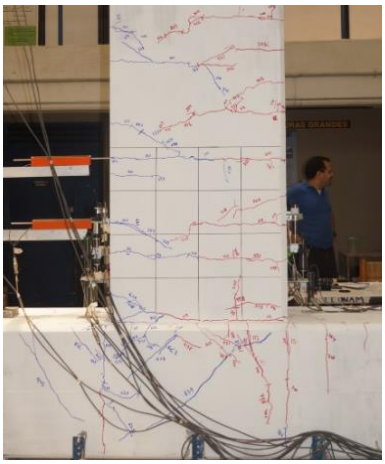

d) Specimen 4 (w_c=2 mm)

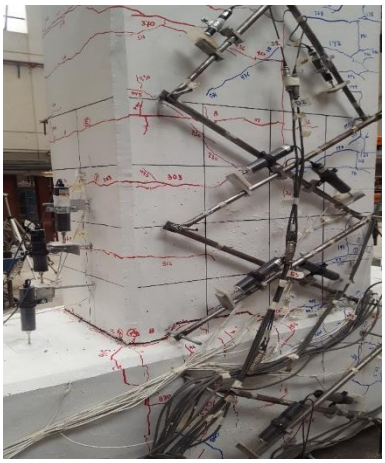

e) Specimen 5 (w_c=1.6 mm)

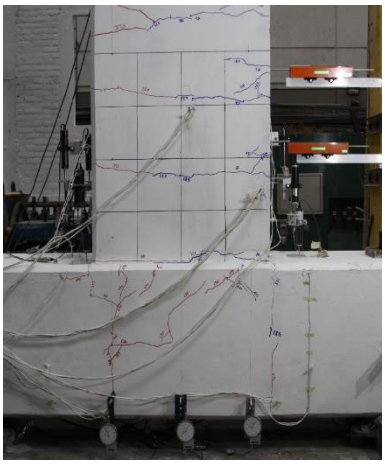

f) Specimen 6 (w_c=1.5 mm)

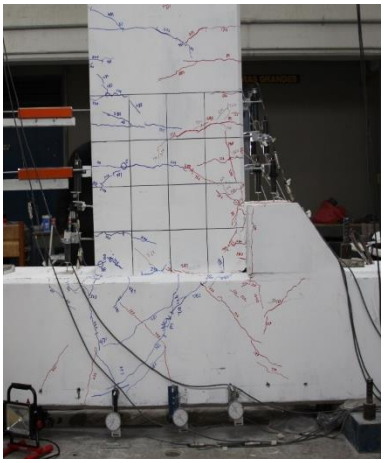

g) Specimen 7 (w_c=1.0 mm)

Figure 4-1. Damage presented on specimens for an inter-story drift of 1%.

a) Specimen 1 (w_c=3 mm)

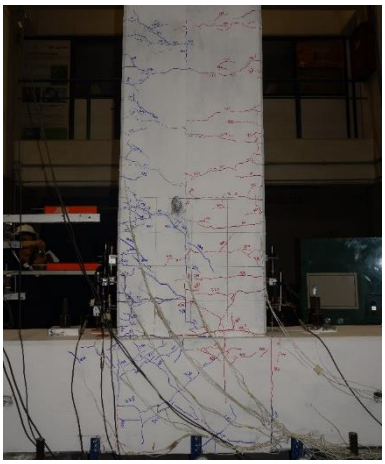

b) Specimen 2 (w_c=4 mm)

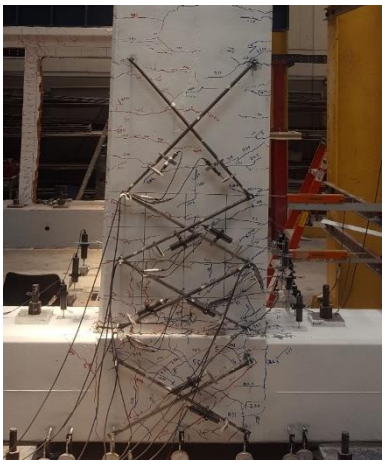

c) Specimen 3 (w_c=4 mm)

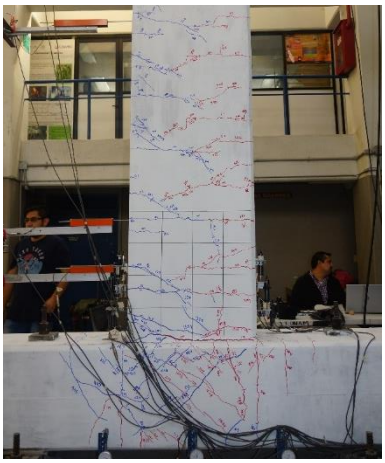

d) Specimen 4 (w_c=3.8 mm)

e) Specimen 5 (w_c=3 mm)

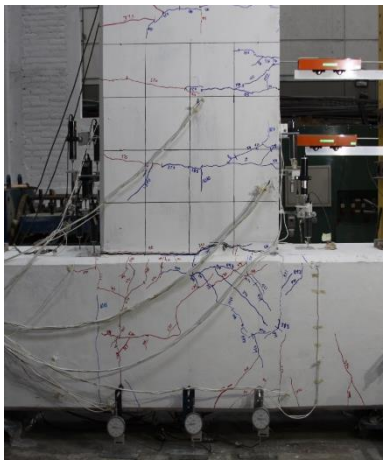

f) Specimen 6 (w_c=3 mm)

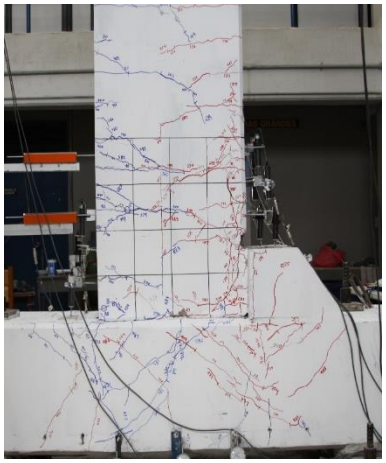

g) Specimen 7 (w_c=3 mm)

Figure 4-2. Damage presented on specimens for an inter-story drift of 2%.

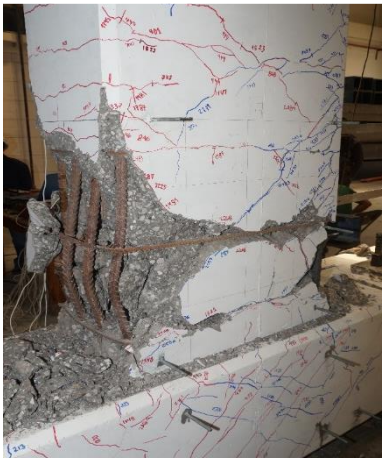

a) Specimen 1 (w_c=5 mm)

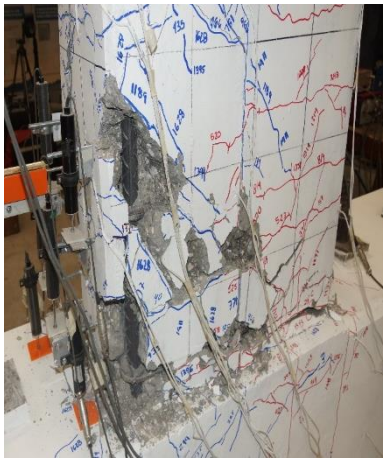

b) Specimen 2 (w_c=8 mm)

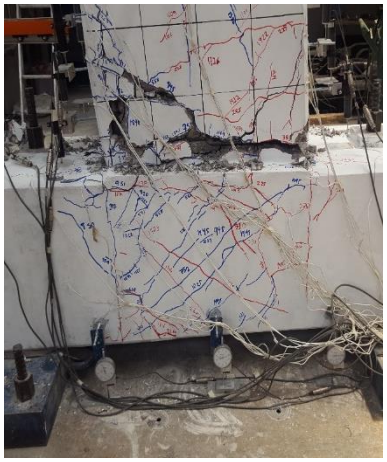

c) Specimen 3 (w_c=8 mm)

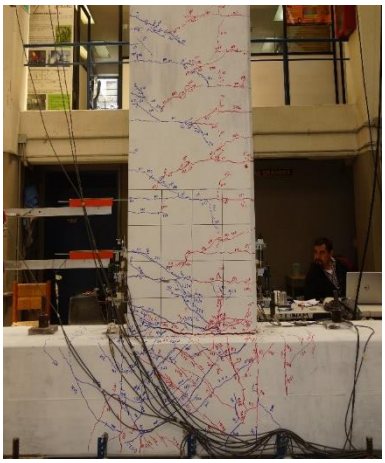

d) Specimen 4 (w_c=7 mm)

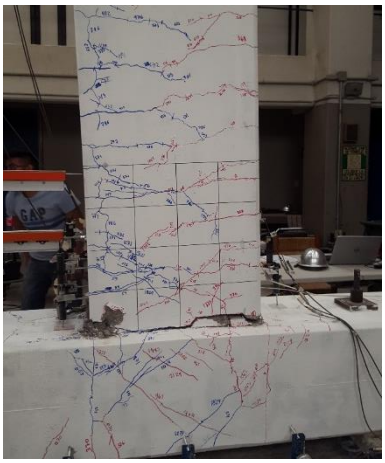

e) Specimen 5 (w_c=6 mm)

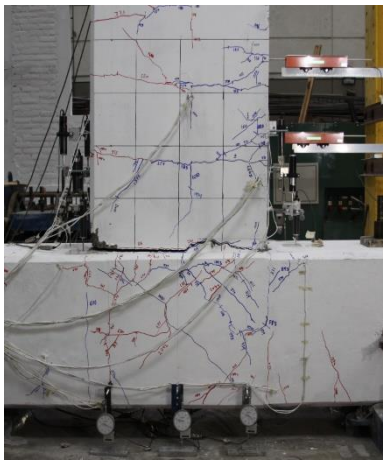

f) Specimen 6 (w_c=6 mm)

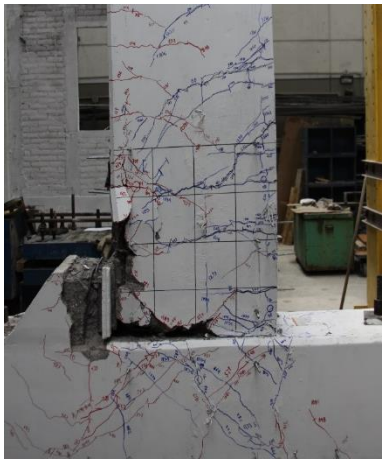

g) Specimen 7 (w_c=7 mm)

Figure 4-3. Damage presented on specimens for an inter-story drift of 3%.

Maximum crack widths for all specimens are shown in Fig. 4-4. It can be seen that propagation of damage was consistent in all specimens at different deformation demands. However, crack widths on Specimens 5 and 6 (post-tensioned) in general were smaller than the other precast specimens. In contrast, Specimen 1 presented the most damage, but with smaller crack widths.

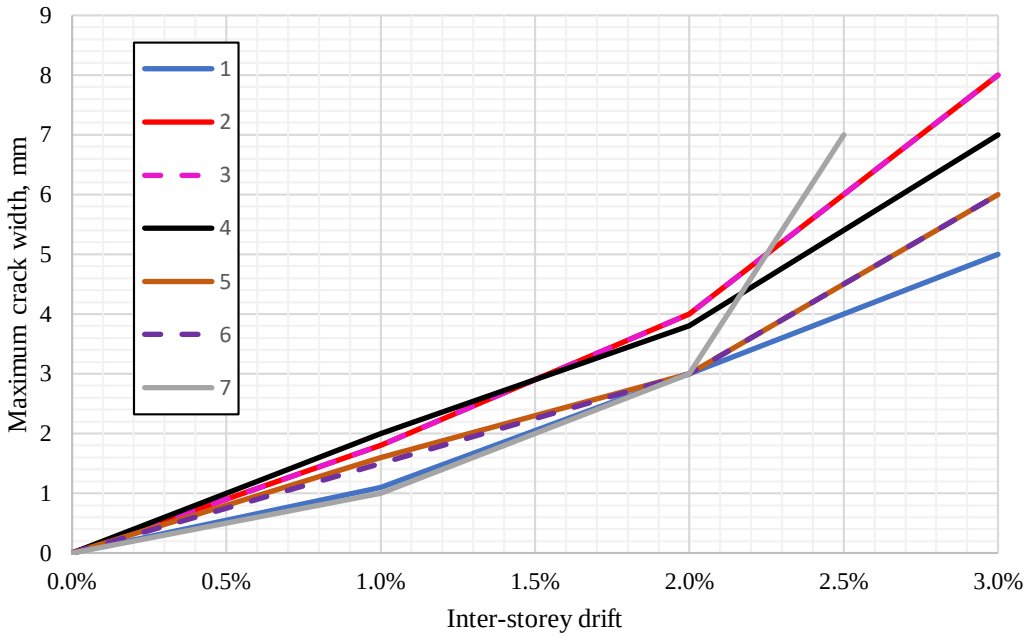

Figure 4-4. Maximum crack width versus inter-storey drift.

4.1 LOAD-DEFORMATION CURVES

Measured load-deformation curves are shown in Figure 4-5. Design strengths, indicated for illustration purposes, were calculated using equations provided by the Mexican City Building Code [4]. Note that the negative design force is smaller in the precast specimens due to the effective depth reduction of the beams bottom steel reinforcement, as mentioned in the experiment setup section. Table 4-1 shows maximum strength (Vu), yielding strength (Vy), maximum displacement (Δ_{max}), yielding displacement (Δy), and ductility (μ) of specimens. Yielding displacement was obtained with specifications from FEMA 356 [33]. Ductility values were calculated as the ratio between the maximum displacement and the yielding displacement.

Some significant observations are worth to be highlighted from Figure 4-5 and Table 4-1:

1. Stiffness of precast specimens were slightly smaller than that of the monolithic connection.
2. In all cases, measured strengths were higher than their corresponding design strengths.
3. Tested specimens yielded at displacements between 40 and 50 mm (or equivalent drifts between 0.8% and 1%).
4. Specimens yielded at strengths similar to those calculated using measured dimensions and material properties.
5. Specimens reached ductility values between 2.5 and 6.2, where ductility was obtained as the ratio between ultimate and measured yielding displacements.
6. Specimens 4, 5 and 6 exhibited pinching behavior close to zero displacement levels.
7. Specimen 4 showed smaller deformation capacity than Specimens 2 and 3 because one of the 90-deg hooks of 2#12 bars fractured at an inter-storey drift to 4.1%. This was attributed to a fabrication imperfection, as the top longitudinal reinforcement was bended with a smaller ratio than that specified by code.
8. Specimen 7 (precast with bracket) showed brittle failure at an equivalent inter-storey drift of 2.5%. The failure occurred in one of the three #10 L-shaped rebars welded to the steel plate PL1 (see Fig. 3.3). The rebar broke just aside plate PL1 were the welding throat started.

Some observations made above can be clearly seen in Fig. 4-6, which shows the envelope hysteresis curves for all specimens. As mentioned, stiffness of the monolithic specimen is slightly higher than the precast elements; all specimens yielded at about 1% inter-storey drift; and the precast specimens reached higher deformation levels than the monolithic specimen, with the exception of specimen 7.

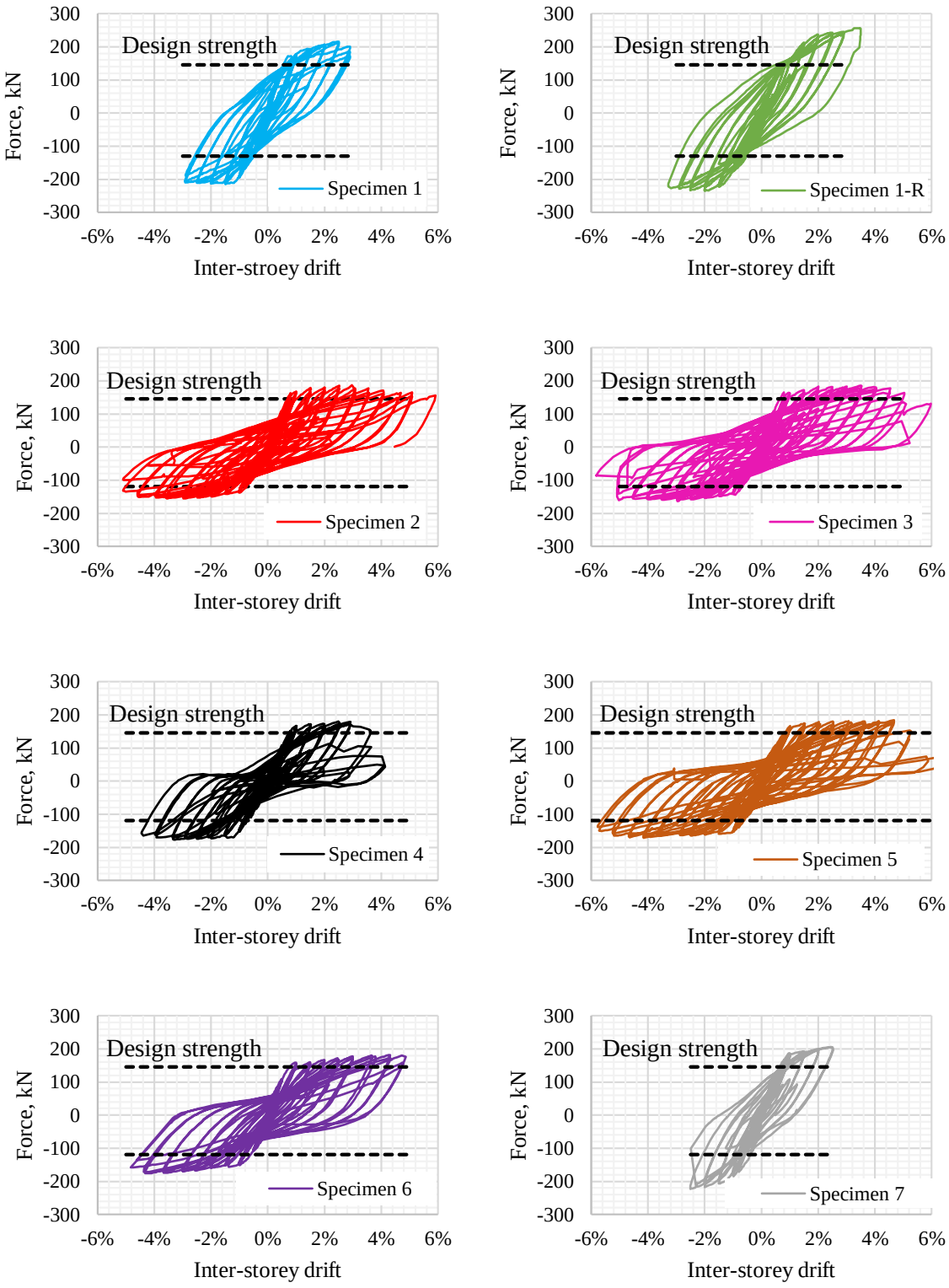

Figure 4-5. Load-deformation curves and calculated strengths.

Table 4-1. Load carrying and deformation capacity.

Specimen	*Vy (kN)*	*Δy (mm)*	*Drift (%)*	*Vu (kN)*	Δ_{max} *(mm)*	*Drift (%)*	*μ*
1	150.9	40.0	0.80	215.1	145.2	2.90	3.63
1-R	158.9	49.7	0.99	256.3	174.8	3.50	3.52
2	164.8	50.3	1.01	186.4	295.8	5.92	5.88
3	162.9	50.2	1.00	185.9	298.9	5.98	5.95
4	167.3	50.3	1.01	180.0	207.1	4.14	4.11
5	160.4	50.9	1.02	184.9	313.0	6.26	6.15
6	147.8	50.1	1.00	197.2	243.6	4.87	4.87
7	181.0	50.0	1.00	234.9	125.8	2.52	2.51

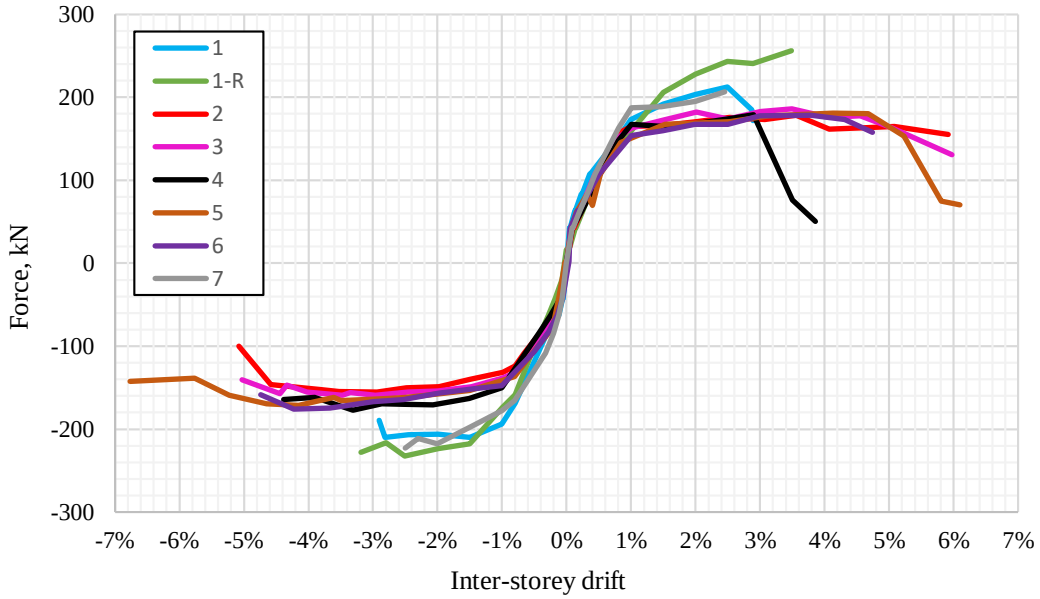

Figure 4-6. Envelope hysteresis curves for all specimens.

4.2 REPAIRED MONOLITHIC SPECIMEN

As mentioned, Specimen 1 was repaired with carbon fiber reinforced polymer (CFRP) jackets on the beam and column next to the joint (Figs. 4-7a to 4-7c). The joint was not rehabilitated. CFRP materials do not corrode and have shown to have excellent fatigue characteristics and very high strength and rigidity in the fiber direction [37]. In durability tests, beams strengthened with CFRP have shown to be susceptible to aggressive environmental

conditions, such as humidity and saltwater solution, that decrease their load-carrying capacity, however, duration of exposure to said conditions have no significant effect on failure loads [38]. In contrast, dry-heat conditions can increase failure loads.

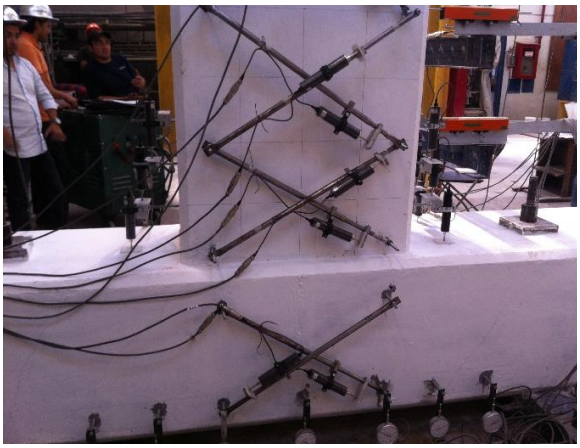

a) Monolithic specimen before testing

b) Monolithic specimen after first test

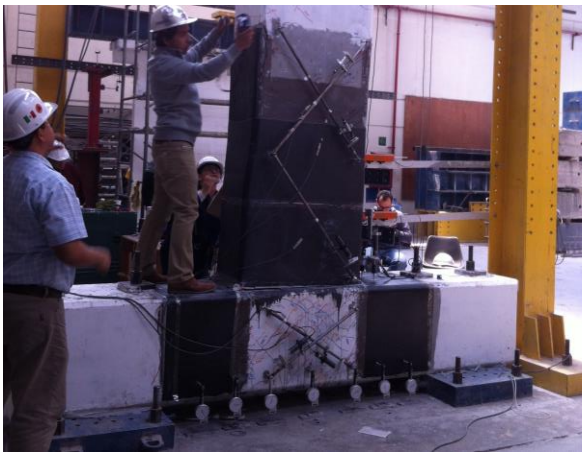

c) Monolithic specimen repaired

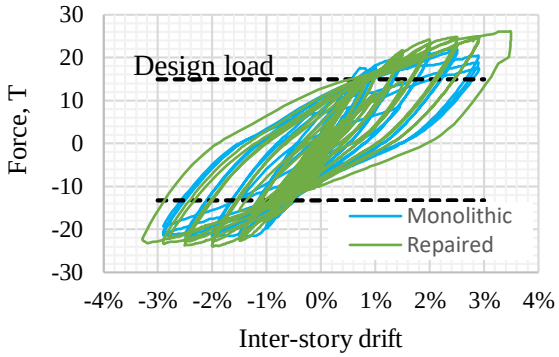

d) Load-deformation curves

Figure 4-7. Specimens 1 and 1-R.

Specimen 1's voids and cavities were filled up with high strength mortar (f'_c=70 MPa) while small cracks (smaller than 2 mm) were injected with epoxy. A comparison of the hysteretic behavior of the monolithic specimen, before repair and after, is shown in Fig. 4-7d. It can be seen that, even though the level of damage after the first test was severe (Fig. 4-7b), the CFRP jacket was effective to recover and even exceed the specimen's original load-carrying capacity. Therefore, it can be concluded that CFRP jacketing (plus the refilling of

cracks with mortar and epoxy) is an effective rehabilitation technique for heavily damaged beam elements.

4.3 ENERGY DISSIPATION

Dissipated hysteretic energy is shown in Fig. 4-8 and the accumulated energy for inter-storey drifts to 1, 2 and 3% (except Specimen 7 that failed at 2.5% drift) are shown in Fig. 4-9. From these graphs, some interesting observations are highlighted:

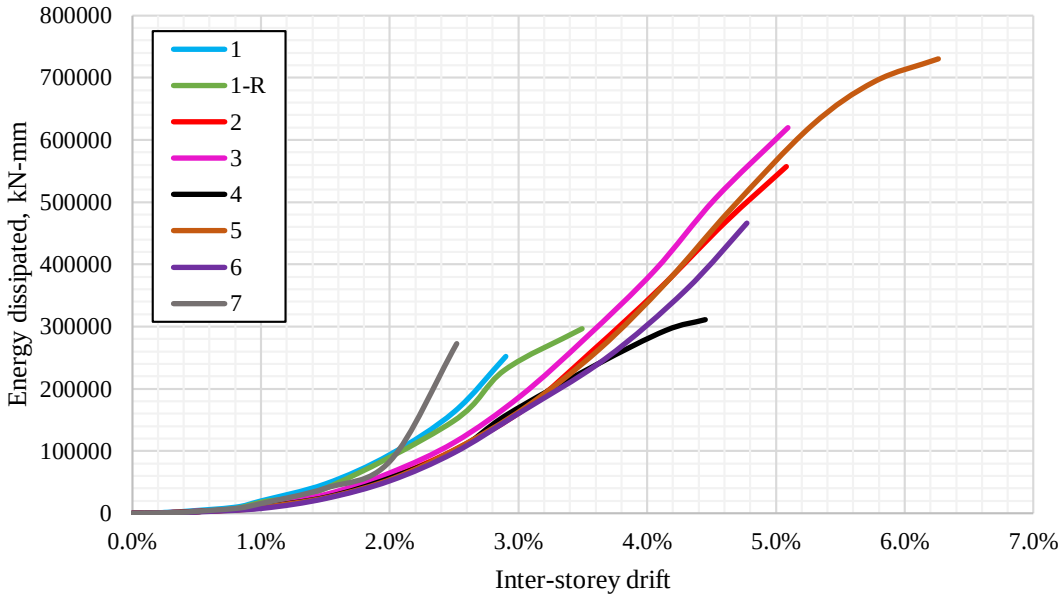

Figure 4-8. Hysteretic energy dissipated by specimen.

1. For inter-storey drifts smaller than 2%, the monolithic specimen (including when repaired) dissipated approximately 40% more energy than their precast counter parts, which can be attributed to excessive cracking.
2. For inter-storey drift ratios between 2 and 2.5%, specimen 7 (with the column bracket) dissipated more energy than the rest of the specimens until failure was observed. This behavior is attributed to large propagation of damage after an inter-storey drift demand of 2%.
3. After a drift ratio of 3%, specimens 2-6 continued dissipating energy, reaching total values as twice as those of the monolithic specimen.

From this section, it can be established that, except for Specimen 7, precast specimens can be taken to higher deformation levels (above 3% inter-storey drift) dissipating a significant amount of hysteretic energy. However, for drift ratios below 3%, their behavior does not match that of Specimen 1. Also, the precast elements (specifically the post-tensioned connections) presented far less damage than the monolithic connection even when taken to drift ratios above 3%.

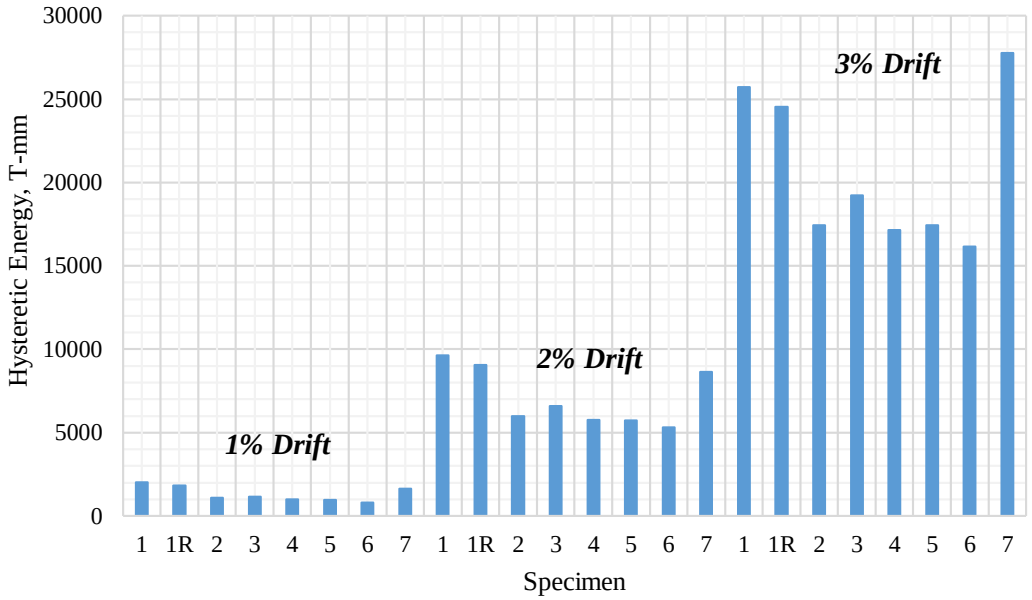

Figure 4-9. Cumulative energy dissipated at inter-storey drifts to 1, 2 and 3%.

4.4 EQUIVALENT VISCOUS DAMPING

The equivalent viscous damping of each specimen up to an inter-storey drift of 3% is presented in Fig. 4-10, and was estimated with Eq. 1 [34]:

$$\xi_{eq} = \frac{1}{4\pi}\frac{E_D}{E_{S0}} \quad (1)$$

where E_D is the energy of the hysteresis loop and E_{S0} is the elastic dissipated energy.

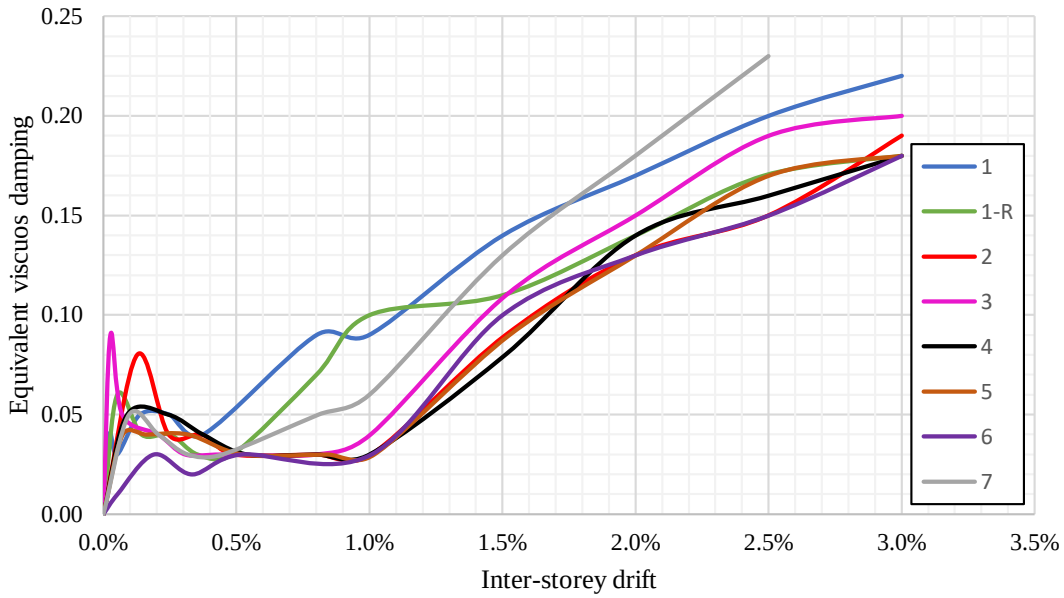

Figure 4-10. Equivalent viscous damping.

Viscous damping of Specimens 5 and 6 is decreased due to the post-tensioned strands closing the cracks when loads are withdrawn. Specimens 1 and 7, that dissipated more hysteretic energy at inte-rstorey drifts to 3 and 2.5% (Fig. 4-8 and 4-9), respectively, are consistent with the calculated equivalent viscous damping in Fig. 4-10. The increased damping on these specimens is attributed to the propagation of damage and the yielding demands on the steel reinforcement. Except for Specimen 7, precast specimens showed similar viscous damping values. Similarities between Figs. 4-9 and 4-10 can be clearly observed, namely: energy dissipation capacity of Specimens 2-6 are consistent and Specimens 1 and 7 dissipated more energy up to inter-storey drifts to 3 and 2.5%, respectively.

CHAPTER 5

EFFECTIVE STIFFNESS

5.1 JOINT AND COLUMN CONTRIBUTION TO STIFFNESS DEGRADATION

Global stiffness of specimens was contributed by beams, joints and columns. However, it was seen during the tests, that damage was concentrated mostly on beams, while cracking of joints and columns was minimal. In order to understand joint and column contribution to stiffness, a linear-elastic analysis was conducted in SAP2000 [30]. Three 2D analysis were conducted (see Fig. 5-1), namely: 1) a beam-column sub-assemblage made of shell elements; 2) a four-storey building made of frame elements; and 3) said building with shell elements.

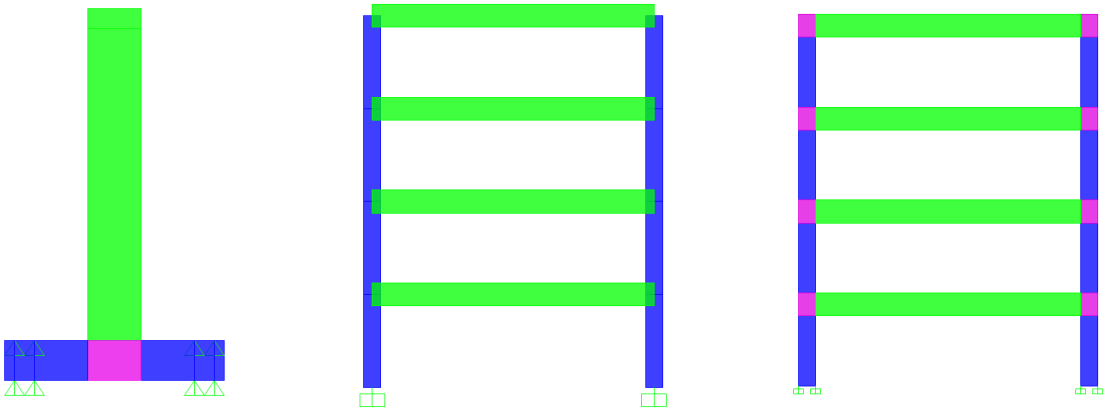

a) Beam-column joint (shell) b) Building (frame) c) Building (shell)

Figure 5-1. 2D models used for analysis.

For the beam-column sub-assemblage (Fig. 5-1a), stiffness was calculated by dividing the force applied horizontally at beam tip by the generated displacement in the same location and direction. For both building models (Figs. 5-1b and 5-1c), stiffness was the division of the applied shear load over the roof displacement. First, an elastic analysis was conducted considering gross sections. After that, elements were affected sequentially, and in

combination, with the stiffness modification factors of Table 2-1, considering ACI-318 [11]. While joints were not considered in the frame building analysis (Fig. 5-1b), their stiffness was reduced with the same factor of 0.7, as used for columns, on the shell models (Figs. 5-1a and 5-1c). Element dimensions and material properties were the same as those tested in this study.

Results of the numeric analysis are shown in tables 5-1, 5-2 and 5-3, where the last column shows the stiffness normalized by that of Analysis 1 (i.e. where full gross sections were considered). It can be observed that applying stiffness reduction factors on joints and columns is not as important as applying them to beam elements. As an example, Analysis 2 of Table 5-3 shows that the model's global stiffness reduces to 0.40 when a stiffness reduction factor of 0.35 is imposed to the beam. On the other hand, Analysis 3 and 4 show that the model's global stiffness kept almost unchanged (above 96%) when stiffness modification factors of 0.7 were imposed to joints and columns. Finally, in Analysis 5, all members were affected with reduction factors and normalized stiffness was similar to Analysis 2, where only beams were affected. Similar effects are seen in Tables 4 and 5.

Table 5-1. Beam-column model made of shell elements.

Analysis	Factored element	Factor	Applied Force, kN	Displacement, mm	k, kN/mm	k_n
1	-	none	1	0.0674	14.83	1.00
2	Beam	0.35	1	0.1701	5.88	0.40
3	Joint	0.7	1	0.0696	14.36	0.97
4	Column	0.7	1	0.0701	14.27	0.96
5	All	0.35, 0.7, 0.7	1	0.1754	5.70	0.38

Table 5-2. Building model made of frame elements.

Analysis	Factored elements	Factor	Total Applied Force, kN	Displacement, mm	k, kN/mm	k_n
1	-	none	4	0.154	25.99	1.00
2	Beams	0.35	4	0.304	13.15	0.51
3	Columns	0.7	4	0.179	22.32	0.86
4	All	0.35, 0.7	4	0.342	11.70	0.45

Table 5-3. Building model made of shells.

Analysis	Factored elements	Factor	Total Applied Force, kN	Displacement, mm	*k*, kN/mm	k_n
1	-	none	4	0.140	28.63	1.00
2	Beams	0.35	4	0.282	14.19	0.50
3	Joints	0.7	4	0.145	27.55	0.96
4	Columns	0.7	4	0.156	25.67	0.90
5	All	0.35, 0.7, 0.7	4	0.314	12.73	0.44

More analysis and discussion could be offered, however, it is evident that beam stiffness plays a significant role on the overall stiffness of the studied models. Because of this, using appropriate stiffness reductions factors on beams is of utmost importance to determine lateral deformations accurately. As will be seen in the following section, experimental evidence shows that beam stiffness is dependent on the imposed deformation and it can be as low as 20% of the elastic stiffness for equivalent inter-storey drift demands close to 1%. This is different to stiffness reduction factors commonly recommended by codes. As a result, an effective stiffness model for estimating beam stiffness at different deformation demands is proposed in section 5.3.

Results of this study, and others (e.g. [1, 10]), demonstrate that code factors underestimate stiffness degradation. Moreover, no inter-storey drift dependence is reflected on these factors.

5.2 STIFFNESS DEGRADATION OF SPECIMENS

Figure 5-2 shows specimen stiffness against the applied inter-storey drift. Experimental values were normalized respect to the elastic stiffness base on gross sections. Calculated elastic stiffness was the same for all specimens because material properties and element dimensions were the same. Measured stiffness was read from the peak-to-peak load-deformation curves corresponding to each small reversal after applying larger deformations. It is significant to mention that stiffness of Fig. 5-2 includes contribution of columns, joints and beams. However, more than 96% of stiffness degradation could be attributed to the beams, as shown in section 5.1.

From Fig. 5-2, although initial stiffness of specimens vary, evident trends are observed. Higher degradation occurred between 0 and 0.5% inter-story drift due to initial cracking; after that, degradation was reduced and varied almost linearly up to 3 and 4%. It is apparent that the monolithic specimen presents a higher stiffness than the rest. Normalized stiffness below 0.20 are seen for inter-storey drift ratios larger than 1%. Note that the precast specimens, which had larger deformation capacity, reached normalized stiffness below 0.10, for very large inter-storey drift demands.

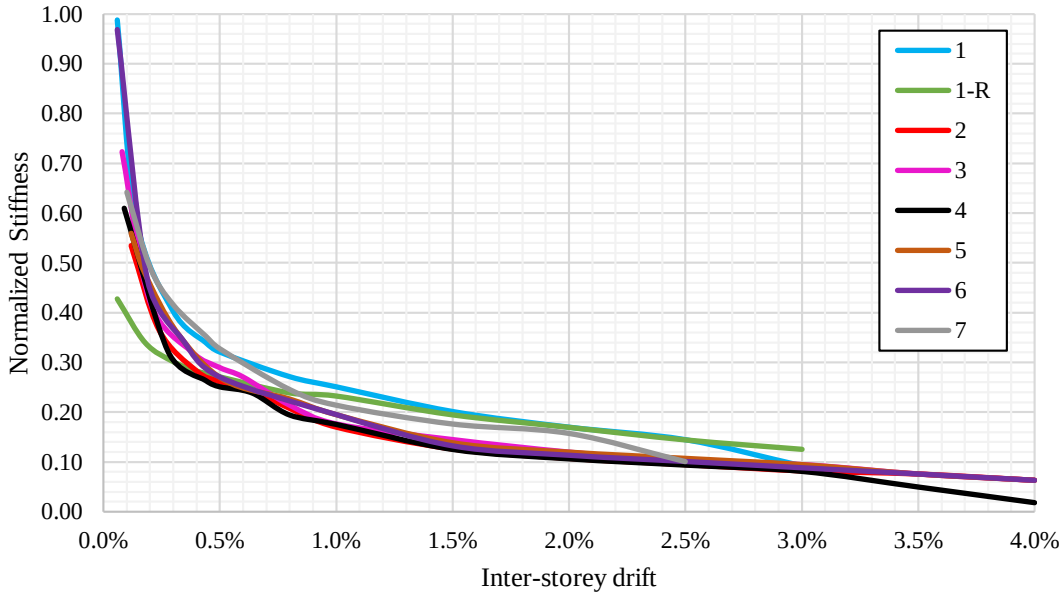

Figure 5-2. Stiffness degradation of tested specimens.

It is significant to note that, up to 0.5% inter-story drift, element stiffness represented on average 28% of the theoretical stiffness. For inter-story drifts of 1, 2 and 3%, element stiffness was 20, 13 and 9%, respectively, of the theoretical stiffness. This raises a significant concern: if for a typical moment resisting frame building, a 2% drift ratio is permitted in ASCE/SEI 7-16 [29] for risk categories I or II, structural sub-assemblages would have undergone an 87% stiffness degradation. ACI-318 [11], however, allows analysis using modification factors of 0.35 and 0.7 of the gross moment of inertia for beams and columns, respectively, as shown in Table 2-1. The MCBC [4], by contrast, recommends a beam cracking factor of 0.5 and 0.7 for columns.

Implications of not properly determining stiffness degradation could be disastrous in some cases. Structures can be left vulnerable to aftershocks and future major earthquakes. Effects could further be amplified if cumulative damage is considered during the structure's life cycle.

5.3 PROPOSED EFFECTIVE STIFFNESS MODEL

Due to noticeable trends of stiffness degradation shown in Fig. 5-1, an effective stiffness model for beam sections is proposed. Such model can be used to predict element stiffness at different inter-story drift demands regardless of the type of beam-column connection. However, it can be refined for different sections or specific connection types if more data was available.

The normalized stiffness of a reinforced concrete beam is defined by the curve shown in Figure 5-3a and estimated with the following equation:

$$k_n = a \cdot \theta^b \ < \ 1 \tag{2}$$

where k_n is the normalized stiffness, a and b are constants that depend on the section type, taken from Table 5-4, and θ is the inter-story drift.

Table 5-4. Values for model constants.

Section Type	**a**	**b**
Monolithic	0.0197	-0.528
Precast	0.0088	-0.636
General	0.0098	-0.626

The expected stiffness can then be calculated with

$$k = k_n \cdot k_g \tag{3}$$

where k_g is the elastic gross cross-sectional stiffness.

Constants for precast elements are valid for precast members with or without post-tensioning. If section type is not an issue, then the general constants can be used, although normalized stiffness of monolithic connections will be underestimated.

In the pursuit of simplicity, a simplified bilinear model is also proposed (Fig. 5-3b) and defined by the following equation:

$$k_n = c\theta + d \tag{4}$$

where k_n and θ were defined above, and the constants c and d are equal to values shown in Table 5-5.

Table 5-5. Values for bilinear model constants.

Drift	c	d
≤0.004	-200	1.0
>0.004	-3.5	0.21

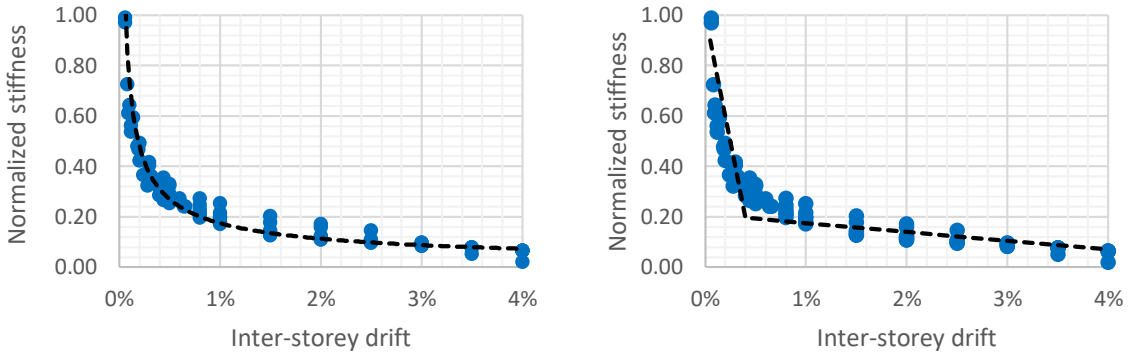

a) Proposed model

b) Simplified bilinear model

Figure 5-3. Proposed Stiffness degradation models.

The proposed models do not take into account the effects of axial loading or amount of longitudinal reinforcement. These effects will be further studied in future investigations.

CHAPTER 6

CONCLUSIONS AND FURTHER WORK

6.1 CONCLUSIONS

Results of an experimental study on precast reinforced concrete beam-column connections were presented in this thesis. Seven specimens were tested: a benchmark monolithic connection, three traditional precast U-shaped connections, two precast post-tensioned hybrid connections and one proposed precast connection supported by a concrete bracket. After the first test, the Specimen 1 was repaired using a fiber reinforced polymer and re-tested. Load-deformation, energy dissipation and stiffness degradation curves were presented, as well as a comparison of the level of cracking under different deformation stages of specimens (equivalent to inter-story drifts of 1, 2 and 3%). Two empirical effective stiffness models were formulated based on the test data: a general model and a simplified bilinear model.

Based on the research findings presented, the following conclusions are drawn:

1. Precast specimens presented slightly smaller stiffness than the monolithic one.
2. All specimens reached higher load capacities than those calculated using design code equations.
3. In terms of load-deformation capacity, the monolithic and precast beams had similar behavior. All specimens yielded at equivalent inter-story drifts between 0.8% and 1% at forces similar to the calculated yielding forces. Ductility ratios ranged between 2.5 and 6.2.
4. Specimens 2-6 showed some pinching behavior close to zero displacement levels.
5. The repaired monolithic connection –using a carbon fiber reinforced polymer jacket and the injection of the cracks with epoxy- recovered its load and displacement capacity despite the severe damage suffered during the first test, which proved this

rehabilitation technique to be adequate.

6. At inter-storey drifts smaller than 3%, the monolithic specimen had a higher energy dissipation capacity due to propagation of damage. After that, precast specimens presented higher deformation and energy dissipation capacity, reaching values as twice as those for the monolithic connection.
7. Precast elements suffered slightly higher stiffness degradation but presented significantly less damage, especially Specimens 5 and 6, than the monolithic specimen.
8. Smaller stirrup spacing favored element performance in terms of observed damage.
9. In terms of cracking, precast specimens exhibited less amount and severity of damage as compared to that of the monolithic specimen. The reduced level of damage can be attributed to the concentration of plastic deformation of beam longitudinal reinforcement at the beam-column interface, where cast-in-place and precast concrete formed a cold joint.
10. Stiffness degradation of specimens was highly dependent on the inter-storey drift demands. These experimental results show that design codes underestimate the effects of cracking on concrete beams. As a result, two empirical effective stiffness models were proposed. No axial load or rebar percentage was considered in the models. The effects of these aspects will be addressed in future studies.

In general, the use of precast concrete beam-column connections have been deemed inefficient in seismic regions, however, results of this study show otherwise. Based on the obtained data, precast connections have reduced stiffness and present slightly more stiffness degradation when compared to cast-in-place connections. On the other hand, they have significantly greater deformation capacity, which effectively leads to greater energy dissipation, similar load carrying qualities and present substantially less damage; properties which are all favorable for seismic design. It can be concluded that the studied precast beam-column connections have acceptable seismic behavior and reasonably emulate monolithic connection.

6.2 FURTHER WORK

Areas for further investigation and development have been identified and are described in this section.

1. As mentioned in Chapter 1, the MCBC and ACI do not separate precast from cast-in-place concrete regarding cracked stiffness modification factors. In Chapter 5, two effective stiffness models for concrete beams is proposed and can be used regardless of section type. Admittedly, the model can be refined if more experimental data were made available. Hence, as an ongoing project at the UNAM, an ideal scenario would be to test more monolithic connections, and different precast connections (including conventional, post-tensioned, and even innovative connections) in order to make an effective distinction between all of them.
2. Challenges in precast construction lie in creating efficient and low cost connections that can replicate or overtake monolithic behavior. Efforts have been made to achieve this and the outcome has been favorable over the last two decades. Specimen 7 was an effort to address the matter of innovation. However, emulative connections seldom progressive beyond prototypes. Therefore, developing non-emulative systems that can exploit the inherent advantages of precast construction can be the alternative we seek.
3. A direct continuation of this study can be the analysis of the discussed precast concrete beam-column connections in two or three dimensional frames subjected to simulated seismic loads including shaking table excitation, which can support the results presented in this thesis. Experimental results such as load-deformation capacity, stiffness degradation, energy dissipation and cracking can be predicted with the results presented in this study and then can be further validated.

Currently, at the UNAM, there are future plans of fabricating and testing new precast connections as a continuation of this study, as well as testing large scale precast buildings equipped with seismic protection systems.

REFERENCES

1. Palmieri L, Saqan E, French C, Kreger M. Ductile Connections for Precast Concrete Frame Systems. Special Publication. 1996; 162.
2. Alcocer SM, Carranza R, Perez-Navarrete D, Martin R. Seismic Test of Beam-to-Column Connections in a Precast Concrete Frame. PCI Journal. 2002.
3. Englekirk RE. Seismic Design of Reinforced and Precast Concrete Buildings. John Wiley and Sons, Inc.: New Jersey, 2003.
4. RCDF, Mexico City Building Code and its Complementary Specifications. 2004: Mexico City, Mexico.
5. RCDF, Mexico City Building Code and its Complementary Specifications. 2017: Mexico City, Mexico.
6. Park HG, Im HJ, Eom TS, Kang SM. An Experimental Study on Beam-Column Connections with Precast Concrete U-Shaped Beam Shells. In: 14th World Conference on Earthquake Engineering. Beijing, China, 2008.
7. Loo YC, Yao BZ. Static and Repeated Load Test on Precast Concrete Beam-to-Column Connections. PCI Journal. 1995.
8. International Federation for Structural Concrete (fib). Structural Connections for Precast Concrete Buildings. Guide to Good Practice. Bulletin 43. 2008.
9. ACI-374.2R-13. Guide for Testing Reinforced Concrete Structural Elements Under Slowly Applied Simulated Seismic Loads. American Concrete Institute: Farmington Hills, MI, USA, 2013.
10. Shariatmadar H, Zamani Beydokhti E. An Investigation of Seismic Response of Precast Concrete Beam to Column Connections: Experimental Study. Asian Journal of Civil Engineering, 2014. Vol. 15; No. 1; 41-59.
11. ACI-318. Building Code Requirements for Reinforced Concrete. American Concrete Institute, 2014.

12. Ruíz-García J, Marín MV, Amador Teran-Gilmore. Effect of Seismic Sequences in Reinforced Concrete Frame Buildings Located in Soft-Soil Sites. Soil Dyn. Earthq. Eng. 63 (2014) 56-68.
13. Guerrero H, Ruíz-García J, J. Alberto Escobar, Amador Teran-Gilmore. Response to Seismic Sequences of Short-Period Structures Equipped with Buckling-Restrained Braces Located on the Lakebed Zone of Mexico City. Eng Struct 2017; 137; 37-51.
14. Astiz L, Kanamori H, Eissler H. Source Characteristics of Earthquakes in the Michoacan Seismic Gap in Mexico. Bull. Seismol. Soc. Am. 77 (1987) 1326-1346.
15. Yuen Kam W, Pampanin S. The Seismic Performance of RC Buildings in the 22 February 2011 Christchurch Earthquake. Struct. Concr. 12 (2011) 223-233.
16. French C, Hafner M Jayashankar V. Connections Between Precast Elements – Failure within Connection Region. Journal of Structural Engineering, American Society of Civil Engineers, V. 115, 1989, 3171-3192.
17. Ochs J, Ehsani M. Moment Resistant Connections in Precast Concrete Frames for Seismic Regions. PCI JOURNAL, V 38, No. 5, 1993, 64-75.
18. El-Sheikh M, Sause R, Pessiki S, Lu L. Seismic Behavior and Design of Unbonded Post-Tensioned Precast Concrete Frames. PCI Journal 1999; 44:54-71.
19. Nakaki SD, Englekirk R, Plaehn J. Ductile Connectors for a Precast Concrete Frame. PCI Journal. 1994.
20. Ertas O, Ozden S, Ozturan T. Ductile Connections in Precast Moment Resisting Frames. PCI Journal. 2006.
21. Parastesh H, Hajirasouliha I, Ramezani R. A new Ductile Moment-Resisting Connection for Precast Concrete Frames in Seismic Regions: An Experimental Investigation. Eng Struct 2014; 70; 144-157.
22. Priestley MJN, Sritharan S, Conley, JR, Pampanin S. Preliminary Results and Conclusions from the PRESSS Five-Story Precast Concrete Test Building. PCI Journal. 1999.
23. Priestley MJN. The PRESSS Program – Current Status and Proposed Plans for Phase III. PCI Journal. 1996.
24. Nakaki SD, Stanton JF, Sritharan S. An overview of the PRESSS Five-Story Precast Test Building. PCI Journal. 1999.

25. Guerrero H, Tianjian Ji, J. Alberto Escobar, Amador Teran-Gilmore. Effects of Buckling Restrained Braces on Reinforced Concrete Precast Models Subjected to Shaking Table Excitation. Eng Struct 2018; 163; 294-310.
26. Guerrero H, Tianjian Ji, Amador Teran-Gilmore, J. Alberto Escobar. A Method for Preliminary Seismic Design and Assessment of Low-Rise Structures Protected with Buckling Restrained Braces. Eng Struct 2016; 123; 141-154.
27. Ghosh, S. K., Nakaki, S.D., and Krishnan, K. Precast Structures in Regions of High Seismicity: 1997 UBC Design Provisions. PCI Journal. 1997.
28. Rivera D, Terrón J, Arce C. Estimación de la Rigidez Agrietada para el Análisis Sísmico en Estructuras de Concreto Reforzado. XIX Congreso Nacional de Ingeniería Estructural. Sociedad Mexicana de Ingeniería Estructural. 2014.
29. ASCE/SEI 7-16. Minimum Design Loads and Associated Criteria for Buildings and Other Structures. American Society of Civil Engineers. 2017.
30. SAP2000. "Structural Analysis Program v19.0.0", Computers and Structures Inc., Berkeley, CA, USA, 2018.
31. Kurose, Y, Guimaraes GN, Zuhua L, Kreger ME, Jirsa JO. Study of Reinforced Concrete Beam-to-Column Joints Under Uniaxial and Biaxial Loading. PMFSEL Report No. 88-2, Phil M. Ferguson Structural Engineering Laboratory, University of Texas at Austin, Austin, Texas, 1988.
32. Ameli MJ, Parks JE, Brown DN, Pantelides CP. Seismic Evaluation of Grouted Splice Sleeve Connections for Reinforced Precast Concrete Column-to-Cap Beam Joints in Accelerated Bridge Construction. PCI Journal, 60 (2), 80-103. 2015.
33. FEMA 356. Federal Emergency Management Agency. "Prestandard and commentary for the seismic rehabilitation of buildings". United States. 2000.
34. Chopra AK. Dynamics of Structures: Theory and Applications to Earthquake Engineering (3th ed.). Prentice-Hall: Upper Saddle River, NJ, 2012.
35. Joshi MK, Murty CVR, and Jaisingh MP. Cyclic Beahaviour of Precast RC Connections. The Indian Concrete Journal, 2005.
36. Park R. The *fib* State-of-the-Art report on the Seismic Design of Precast Concrete Building Structures. Pacific Conference on Earthquake Engineering, 2003.

37. Issa CA and AbouJouadeh A. Carbon Fiber Reinforced Polymer Strengthening of Reinforced Concrete Beams: Experimental Study. ASCE Journal of Architectural Engineering, 2004.
38. Grace NF and Singh SB. Durability of Carbon Fiber-Reinforced Polymer Strengthened Concrete Beams: Experimental Study and Design. ACI Structurak Journal, No. 102-S05, 2005.